applied sciences

MDPI

Review

Synthesis of Micro- and Nanoparticles in Sub- and Supercritical Water: From the Laboratory to Larger Scales

F. Ruiz-Jorge, J. R. Portela *, J. Sánchez-Oneto and E. J. Martínez de la Ossa

Department of Chemical Engineering and Food Technology, Faculty of Sciences, University of Cádiz, 11510 Puerto Real (Cádiz), Spain; franciscojavier.ruiz@uca.es (F.R.-J.); jezabel.sanchez@uca.es (J.S.-O.); enrique.martinezdelaossa@uca.es (E.J.M.d.l.O.)

* Correspondence: juanramon.portela@uca.es

Received: 30 June 2020; Accepted: 6 August 2020; Published: 9 August 2020

Featured Application: This review on hydrothermal particle synthesis is mainly oriented to new researchers or research groups that are attracted by the promising future of this technology. This review gives an interesting overview.

Abstract: The use of micro- and nanoparticles is gaining more and more importance because of their wide range of uses and benefits based on their unique mechanical, physical, electrical, optical, electronic, and magnetic properties. In recent decades, supercritical fluid technologies have strongly emerged as an effective alternative to other numerous particle generation processes, mainly thanks to the peculiar properties exhibited by supercritical fluids. Carbon dioxide and water have so far been two of the most commonly used fluids for particle generation, the former being the fluid par excellence in this field, mainly, because it offers the possibility of precipitating thermolabile particles. Nevertheless, the use of high-pressure and -temperature water opens an innovative and very interesting field of study, especially with regards to the precipitation of particles that could hardly be precipitated when CO_2 is used, such as metal particles with a considerable value in the market. This review describes an innovative method to obtain micro- and nanoparticles: hydrothermal synthesis by means of near and supercritical water. It also describes the differences between this method and other conventional procedures, the most currently active research centers, the types of particles synthesized, the techniques to evaluate the products obtained, the main operating parameters, the types of reactors, and amongst them, the most significant and the most frequently used, the scaling-up studies under progress, and the milestones to be reached in the coming years.

Keywords: hydrothermal synthesis; supercritical fluids technology; particle synthesis; subcritical and supercritical water; micro- and nanoparticles; scale-up

1. Introduction

The fluids at high pressure and temperature that are most frequently used for the industrial processes are carbon dioxide (CO_2) and water (H_2O), mostly because they can be acquired easily and economically. These fluids, like any other fluid, are characterized by a specific critical pressure and temperature and when those conditions are exceeded, they reach supercritical state. When the supercritical state is reached, liquids exhibit properties that are between those of a liquid and a gas (their diffusivity is near that of a gas and their solvent capacity is similar to that of a liquid, among others) [1]. These characteristics fit ideally with those required for several industrial processes. With regards to CO_2 and H_2O, some examples of the main high-pressure and -temperature applications that have been developed so far are the following:

For CO_2

- Impregnation of matrices with antioxidant particles [2,3].
- Fabrication of biodegradable polymeric [4].
- Precipitation of antioxidants from natural extracts using CO_2 as solvent and antisolvent [5,6].
- Precipitation of metallic nanoparticles [7].
- Extraction and fractionation of substances of interest using CO_2 as solvent [8].

For H_2O

- Wet oxidation and oxidation with supercritical water [9,10].
- Hydrothermal liquefaction [11].
- Gasification with supercritical water [12].
- Cooling down nuclear reactors [13].
- Precipitation of micro- and nanoparticles [14,15].

As can be seen extensively in the literature [5–7,14,15], high-pressure and -temperature fluids turned into a significant tool to synthesize and precipitate micro- and nanoparticles of great interest and that may have variations in morphology and size that may determine the potential in the implementation of these technologies.

CO_2 is the most frequently used fluid to produce reduced-size particles (nano and micro), mainly because of its relatively low critical pressure and temperature (73.8 bar and 31.1 °C, respectively), which makes of this an economically feasible procedure when compared to others that use other fluids. It also offers the possibility of precipitating thermolabile particles. Consequently, and based on the promising qualities showed by CO_2, this procedure was the subject of many and thorough studies where different technologies that use CO_2 as the solvent, antisolvent, or reagent were developed, as can be seen in the review by Kankala et al. [4].

Like carbon dioxide, water also opens an interesting field of study, particularly on the precipitation of particles which may encounter certain difficulties when CO_2 is used. For instance: metal particles of a considerable value in the market. The excellent properties of water, for the production of nano- and microparticles, as its thermophysical properties (see Section 2), made it the focus of attraction and interest for new research groups, who probably find this synthesized review on the hydrothermal synthesis of particles very useful, since it has a wide field of study that encompasses the entire range production scenarios, from a small scale (initial investigation phases) to a pilot plant scale. Furthermore, this review describes essential sections for new research groups, such as the differences between this method and other conventional procedures, the most currently active research centers, the types of particles synthesized, the techniques to evaluate the products obtained, and the main operating parameters and deals extensively with what is still to be investigated as well as prospective trends in the near future.

Hydrothermal synthesis is a branch in hydrothermal technology that is currently opening new perspectives, as can be seen in Figure 1. It links all the relevant technologies such as biotechnology, nanotechnology, and advanced materials technologies [16].

A clearly growing demand for nanotechnology and advanced material technologies boosted the interest on hydrothermal synthesis processes over the last 15 years. Carrying out an intensive search in the SCOPUS database, filtering and classifying later, it was possible to construct Figure 2. As can be seen from Figure 2, despite the 1997 and 2008 economic recessions, a growing number of research articles were published from the year 1987 until the year 2020. According to refined data, China represents 32.07% of the total number of articles published, followed by USA (5.2%), Japan (4.9%), and India (3.9%).

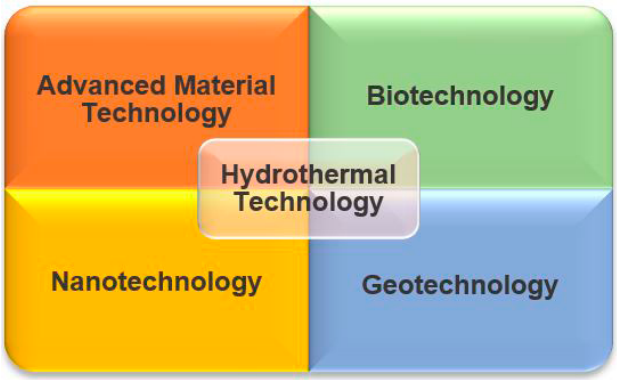

Figure 1. Hydrothermal technology in the 21st century.

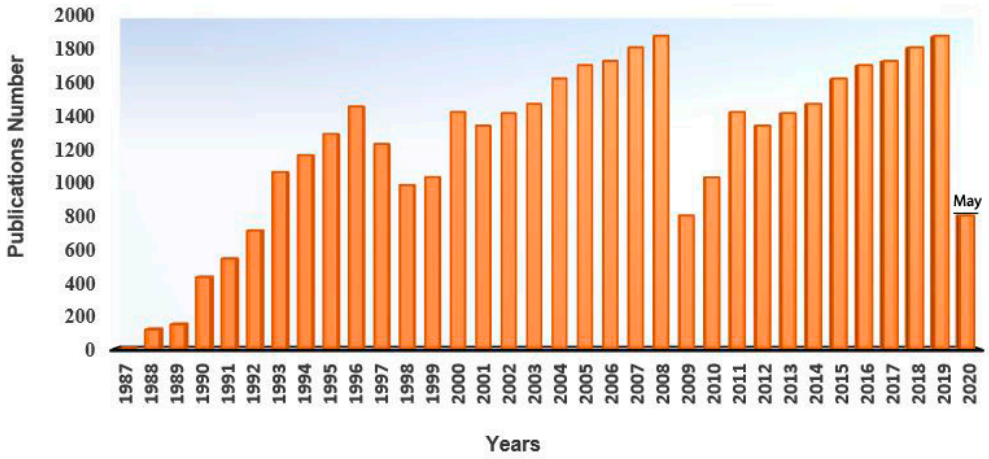

Figure 2. Evolution of the number of publications on hydrothermal synthesis from January 1987 until May 2020.

The gradual growth of publications on hydrothermal synthesis is due mainly to the fact that solvent used like reaction medium, distilled or millipore water in the majority of cases, is an easy-to-obtain solvent; it is environmentally friendly, harmless for human beings, non-flammable, and totally recyclable [13]. Another relevant feature is the reproducibility of the process and its capacity to generate pure particles with narrow size variations and a substantial variability of morphologies. As can be seen in Section 3.2, the industrial applications of the synthesized particles are numerous and include catalysis, energy storage, biomedicine, etc.

The term "hydrothermal" has geological origin. It was used for the first time by the British Geologist Sir Roderick Murchison (1792–1871) to describe the changes that water at high temperature and under high pressure caused on the Earth's crust, which leads to the formation of several rocks and minerals [17]. Hydrothermal or hydrothermal synthesis can be classified under the solvothermal synthesis category, that comprises any process by which particles are generated in the presence of a solvent while temperature is above ambient temperature and at pressure above 1 atm. Therefore, the hydrothermal reactions for the formation of particles are solvothermal reactions where water is used as a solvent. Authors such as Professors F. Cansell and Cyril Aymonier, from the Institute of Chemistry and the Condensed Matter (Bordeaux) and M. Poliakoff from the University of Nottingham (UK), completed numerous studies on the precipitation of nanoparticles using fluids such as acetone, hexane, or even a supercritical mixture in water; seeking a greater crystallization of the particles at lower temperatures, because the critical parameters of the mixtures are usually lower than those of pure water [18,19].

For a better understanding and control of the hydrothermal process, it is necessary to be familiar with water properties according to temperature and pressure. Water supercritical point is of particular relevance, i.e., the point where water turns from subcritical into supercritical water; that is to say 221 bar and 374 °C.

Figure 3 shows the phases diagram for pure water. Along the vaporization curve, as pressure and temperature increase, intermolecular interactions in the fluid decrease due to thermal expansion. On the other hand, the effect of compression prevails on the vapor phase against thermal expansion and intermolecular interactions increase. This makes the properties of the fluid and the vapor get closer until the critical point is reached, where water turns into supercritical state.

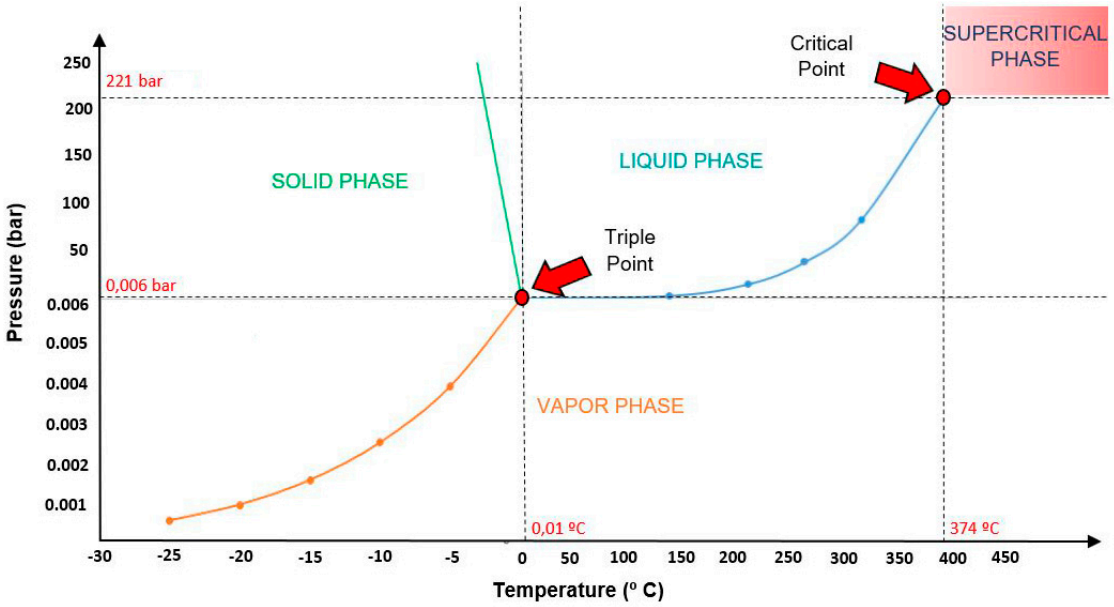

Figure 3. Water phases diagram.

2. Water Properties

Water properties when conditions are below water's critical point have been thoroughly studied, but those properties which water acquires when approaching its critical point are the ones to provide water with optimum capacity for particle precipitation purposes. It is, therefore, necessary to understand the basic principles of the different water properties such as: density, viscosity, specific heat, thermal conductivity, and dielectric constant when conditions are near water's critical point.

2.1. Density

Figure 4 represents pure water's density diagram as function of temperature under different pressure levels according to the data provided by the NIST (National Institute of Standards and Technology). It can be seen that when near the critical point, the density strongly varies with pressure, since as water approaches its critical point, its compressibility becomes infinite.

In the regions near its critical point, water density drops drastically, which affects salt solubility and in turn leads to oversaturation and nucleation of the particles.

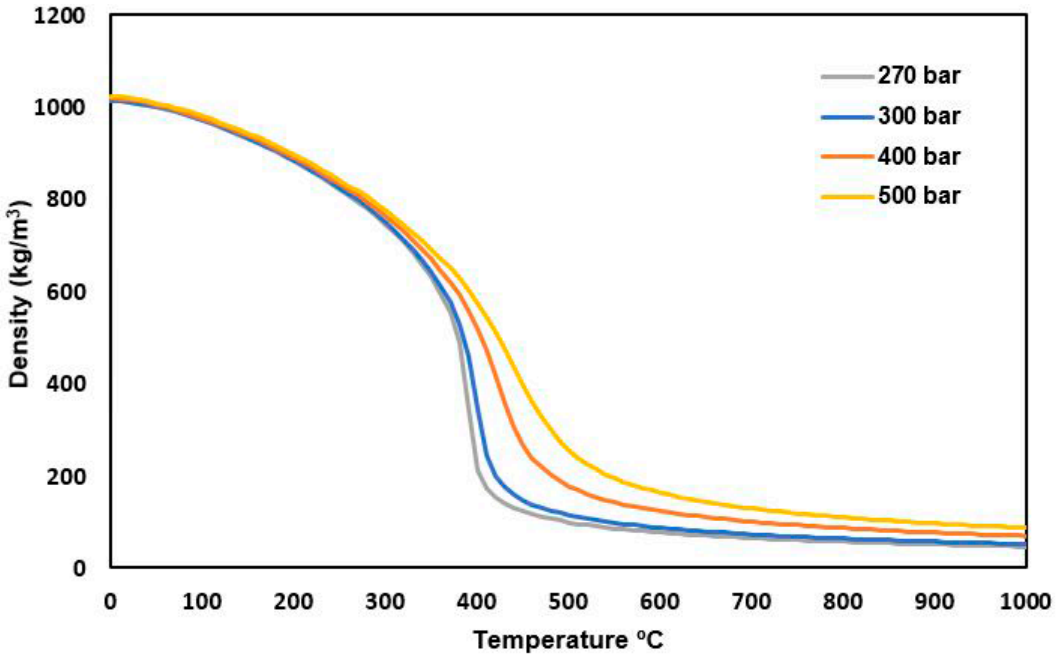

Figure 4. Water density variation with temperature under different pressure levels. (Plotted according to the data provided by the National Institute of Standards and Technology (NIST; www.nist.gov; 10 June 2020)).

2.2. *Viscosity*

Figure 5 represents the viscosity diagram of pure water as a function of temperature under different pressure levels based on the data provided by the NIST. It can be seen that, similarly to what happens to density, pressure has a greater influence on viscosity than temperature when water is near its critical point.

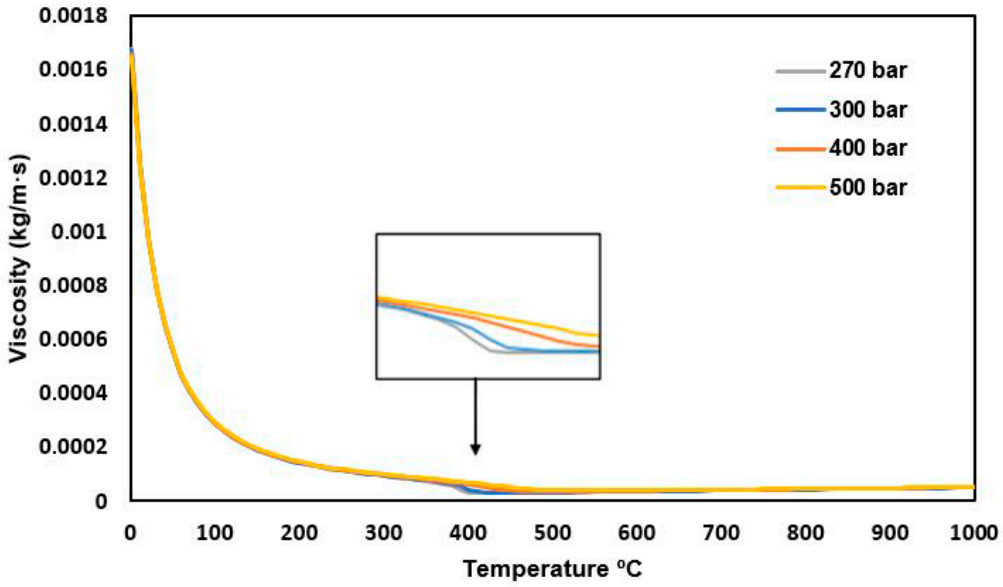

Figure 5. Water viscosity variation with temperature under different pressure levels. (Plotted according to the data provided by the NIST (www.nist.gov; 10 June 2020)).

At the critical point, viscosity drops one order of magnitude with respect to liquid water, and therefore, there is an increment in its diffusion coefficient and ionic mobility values, which in turn increments its reaction rate.

2.3. Specific Heat

Figure 6 represents the calorific value diagram of pure water as a function of temperature under different pressure levels based on the data provided by the NIST. It can be seen how the calorific value of water varies within a wide range of pressure and temperature levels and reaches it maximum point when near its critical point because of the significant thermal expansion of water at phase transition. Due to the considerable increment in the specific heat of water as it approaches the critical point, there is an enormous demand for energy to go beyond such critical point. This makes hydrothermal synthesis, as well as the rest of the hydrothermal procedures, a technology with a substantial financial toll.

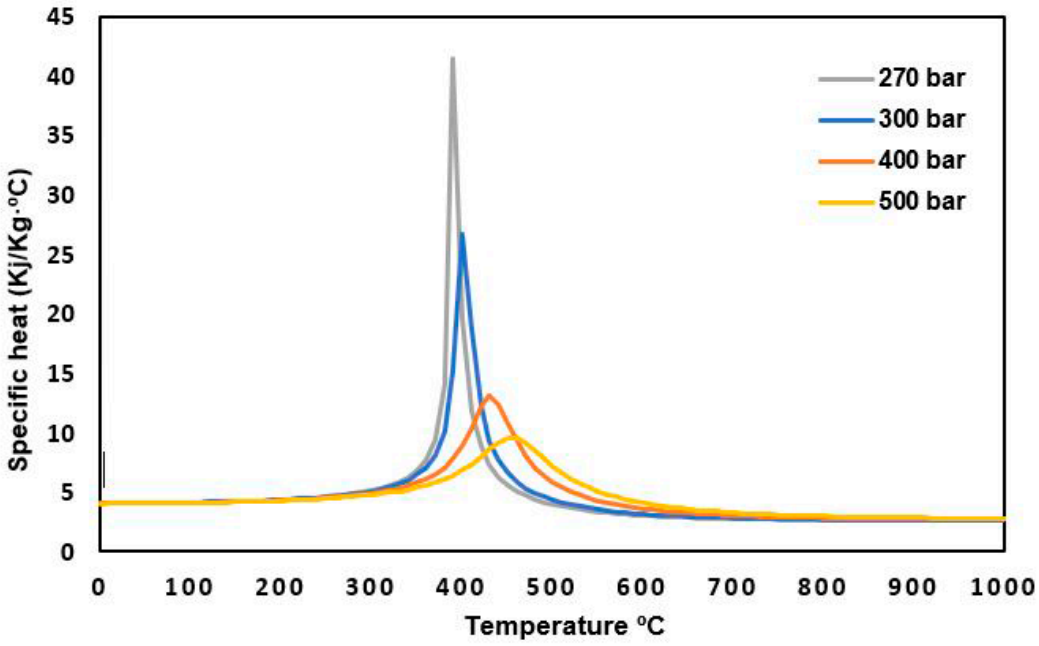

Figure 6. Water-specific heat variation with temperature under different pressure levels. (Plotted according to the data provided by the NIST (www.nist.gov; 10 June 2020)).

2.4. Thermal Conductivity

Figure 7 represents the conductivity diagram of pure water as a function of temperature under different pressure levels. It can be seen that water conductivity, at constant pressure, increases as the temperature goes up until near the critical point, where a rapid drop occurs.

Low thermal conductivity near the critical point may pose a serious problem when working with large volume reactors. Temperature gradients would be very likely generated, and undesired compounds would appear together with a great distribution of particle sizes.

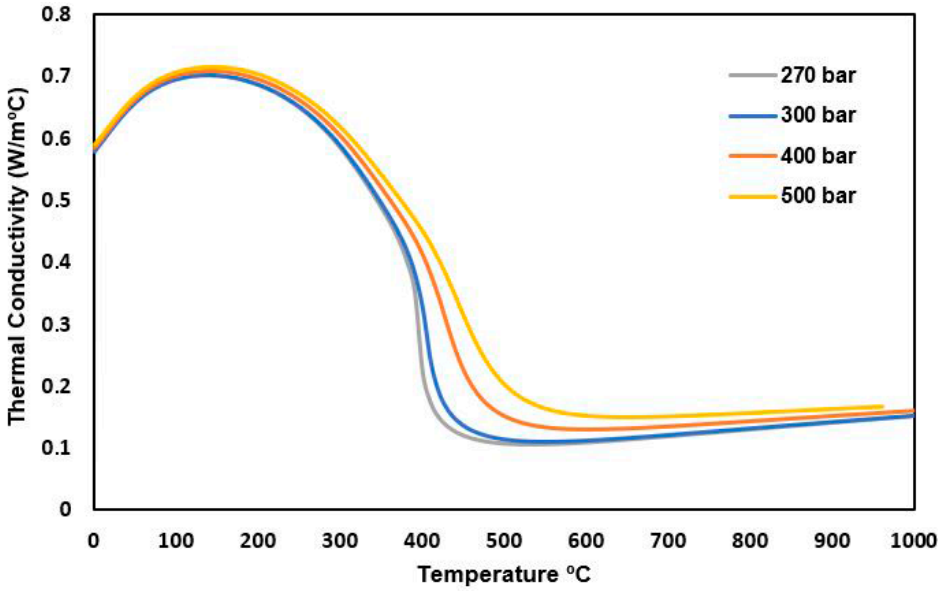

Figure 7. Water thermal conductivity variation with temperature under different pressure levels. (Plotted according to the data provided by the NIST (www.nist.gov; 10 June 2020)).

2.5. Dielectric Constant and Ionic Product

Water's dielectric constant as well as its ionic product determine its behavior as a solvent for the ionic dissociation of salts. Water's dielectric and dissociation constant diagrams show how its dielectric constant decreases and its dissociation constant increases as temperature and density increase [20]. This causes water above its critical point to behave more like a non-polar solvent than a polar solvent, considerably affecting hydrolysis of the metal salt, and generating an oversaturation and nucleation of particles (see in more detail in Section 3).

The fact that, under these conditions, water turns into a non-polar solvent opens a promising field of study based on the generation of hybrid metal-organic particles which could be mainly applied to medical purposes.

In order to sum up and as a quick guide of the changes that water properties show as conditions vary, Table 1 shows the specific values of water physicochemical properties depending on the hydrothermal operating conditions applied to the precipitation of micro- and nanoparticles.

Table 1. Water Properties under Different Pressure (P) and Temperature (T) levels.

Properties	Environmental Conditions (25 °C and 1 bar)	Subcritical Conditions (325 °C and 200 bar)	Supercritical Conditions	
			(525 °C and 250 bar)	650 °C and 250 bar)
Density (kg/m^3)	997.1	679.8	83.5	64.8
Viscosity (μPa·s)	890.1	80.5	31.6	36.4
Specific heat (J/g·K)	4.2	6.0	3.5	2.0
Dielectric constant	78.4	18	2.5	2.5
Thermal conductivity (W/m·K)	0.6	0.5	0.01	0.1

It has been clearly established the critical point of water as the point at which water turns into a supercritical state or vice-versa, and it is of the utmost importance for hydrothermal synthesis processes. Nevertheless, it is also important to point out that these data correspond to pure water and that, generally, concentrated solutions are used for hydrothermal synthesis, which would make the critical point shift to a greater or lesser extent [17].

3. Micro- and Nanoparticles Generating Procedure in Sub- and Supercritical Water

The usage of micro- and nanoparticles in chemical, pharmaceutical, or material industries is clearly booming, due to their mechanical, chemical, physical, electrical, optical, and thermal properties, provided by their high surface volume ratio and its peculiar shapes and structures in space [21]. The exclusive properties of micro- and nanoparticles make them widely usable for different technologies associated to ceramic, catalysis, data storage, biomedicine, pharmacy, energy, etc.

Generally, the different particles are obtained by physical or chemical processes [22], including several techniques in each case, as the examples shown below:

Physical Processes

- Thermal evaporation [23]
- Gas clusters preparation [24]
- Ion implantation [25]
- Chemical vapor deposition [26]
- Grinding or mechanical-chemical activation [27].

Chemical Processes

- Radiolytic and photochemical reduction [28]
- Microwave irradiation [29]
- Solvothermal synthesis [30]
- Sol–gel process [31].

When compared to other conventional methods, the process to generate micro- and nanoparticles is favored when the precipitation is generated by means of near or supercritical water. This is due to the above-mentioned water properties, which provide a greater control of the nucleation, a greater reaction rate and an improved control of the particles shapes. Furthermore, they can be carried out by means of relatively simple and low-volume equipment [21].

The reactions that take place in hydrothermal synthesis are still to be thoroughly determined and studied. This is mainly due to lack of data on intermediate compounds. It is true that a large number of particle types implies some difficulties to develop the appropriate software application that may generate reliable predictive models, since each particle type may have its own intermediate compounds and crystallization rate.

Failing to count on such predictive models, the influence of temperature, pressure, precursor, and time on the crystallization kinetics of the different compounds should be empirically determined. By getting to know how these variables work, we should learn how to control particle formation, their purity, formation time, and operating conditions [16].

The best approach in recent years to this problem was based on four simple steps [16]:

1. Calculating the thermodynamic equilibrium as a function of the process variables.
2. Generating the equilibrium diagrams to map the phases of interest of the process variables.
3. Designing hydrothermal experiments to test and validate the diagrams previously calculated.
4. Using the process variables to control the reactions and the crystallization kinetics.

In this way, a bidimensional phase diagram would be obtained by varying the media pH while the precursors concentration, temperature and pressure would remain constant. This would allow to determine the type of particle that would be generated and its purity depending on the pH value [32]. The diagrams can also be three-dimensional, that is, relating three of the variables mentioned, such as pH, temperature, and purity.

Going deeper in this subject, Professor Adschiri et al. [16] already completed some studies on the line of reactions. They hold that two types of reactions take place during the simple oxides forming process. The former is hydrolysis (Equation (1)) and the latter is dehydration (Equation (2)). First, the

metal salt is hydrolyzed into metal hydroxide. Then it is immediately precipitated as metal oxide by dehydration due to its low solubility in water under hydrothermal conditions.

$$M(NO_3)_2\ (s) + xH_2O\ (l) \rightarrow M(OH)_x\ (s) + xHNO_3\ (l) \quad (1)$$

$$M(OH)_x\ (s) \rightarrow MO_{x/2}\ (s) + \frac{x}{2}H_2O\ (l) \quad (2)$$

Metal oxides' low solubility is due to water's density drop and dielectric constant variations of water when near the critical point (see Table 1).

Below some examples of very active authors in recent years with regards to hydrothermal synthesis are named, the centers they work for, and some of their most recent papers. The types of generated particles and their more characteristic morphology of particle will also be mentioned.

3.1. Research Centers

Many authors all over the world completed extensive studies on the precipitation of crystalline micro- and nanoparticles using different reactor types. Table 2 shows some of the most prolific authors with regards to hydrothermal synthesis in the last few years, the organizations they work for, and some of their studies.

Table 2. Some of the most prolific authors associated to hydrothermal synthesis in the last few years and the organizations they work for.

Principal Investigators	Research Centers	Articles
United States		
Zubieta, John A.	Syracuse University, Syracuse	[33,34]
Whittingham, M. Stanley	Binghamton University State University of New York, Binghamton.	[35,36]
Komarneni, Sridhar	University Park, The Pennsylvania State	[37]
Kolis, Joseph W.	Clemson University, Clemson	[38,39]
China		
Yang, Guoyu	Beijing Institute of Technology, Beijing	[40,41]
Hu, Changwen	Beijing Institute of Technology, Beijing	[42,43]
Zeng, Wen	Chongqing University, Chongqing	[44,45]
Feng, Shouhua	Jilin University, Changchun	[46,47]
Cui, Xiaobing	Jilin University, Changchun	[48,49]
Shi, Zhan	Jilin University, Changchun	[50,51]
India		
Byrappa, Kullaiah K.	University of Mysore, Vijnana Bhavan, Mysore	[52,53]
Natarajan, Srinivasan	Indian Institute of Science, Bengaluru	[54,55]
Pandurangan, Arumugam	Anna University, Chennai	[56,57]
Patil, Pramod Shankarrao	Shivaji University, Kolhapur	[58,59]
Japan		
Yanagisawa, Kazumichi	Kochi University, Kochi	[60,61]
Adschiri, Tadafumi	Tohoku University, Institute for Materials Research, Sendai	[62,63]
Yoshimura, Masahiro	Tokyo Institute of Technology, Tokyo	[64,65]
Takami, Seiichi	Nagoya University, Nagoya	[66,67]
Yin, Shu	Tohoku University, Sendai	[68,69]
Hakuta, Yukiya	National Institute of Advanced Industrial Science and Technology, Tokyo	[70,71]
Hirano, Masanori	Aichi Institute of Technology, Toyota	[72,73]
Iran		
Salavati-Niasari, Masoud	University of Kashan, Kashan	[74]
Haghighi, Mohammad	Sahand University of Technology, Sahand	[75]

Table 2. *Cont.*

Principal Investigators	Research Centers	Articles
Europe		
Stock, Norbert	Christian-Albrechts-Universität zu Kiel, Kiel, Germany	[76]
Klingeler, Rüdiger	Universität Heidelberg, Heidelberg, Germany	[77,78]
Darr, Jawwad Arshad	University College of London, London, United Kingdom	[79,80]
Walton, Richard I.	The University of Warwick, Coventry, United Kingdom	[81,82]
Lester, Edward Henry	Nottingham University, United Kingdom	[83,84]
Brummerstedt Iversen, Bo	Aarhus Universitet, Aarhus, Denmark	[85,86]
Cyril Aymonier	The Institute of Condensed Matter Chemistry of Bordeaux, CNRS and Bordeaux University, France	[87,88]
Russia		
Ivanov, Vladimir K.	Kurnakov Institute of General and Inorganic Chemistry, Russian Academy of Sciences, Moscow	[89,90]
Taiwan		
Chen, Shenming	National Taipei University of Technology, Taipei, Taiwan	[91]
Australia		
Wang, Guoxiou Xiu	University of Technology Sydney, Sydney	[92,93]

Amongst all the above mentioned author, Professors Arai and Adschiri from the University of Tohoku (Japan) stand out as pioneers in this field, mainly for their numerous and innovative studies on the precipitation of nanoparticles in continuous reactors that allow an improved control of the experimental conditions and, therefore, the production of particles of smaller and constant size [94]. In this same field of continuous particle precipitation, Professor J. Darr from University College of London and Professors M. Poliakoff and E. Lester from the University of Nottingham (United Kingdom) also stand out. As will be further detailed in Section 5.3 below, the University of Nottingham is leading a project for the scaling up of hydrothermal synthesis processes.

The researcher L. Kashinath and Professor K. Byrappa from the University of Mysore (India) carried out an interesting study on a microwave-assisted hydrothermal method aiming to set up a new way to study the synthesis, interaction, kinetics, and mechanisms of the hybrid nano-compound formed by zinc oxide on graphene oxide sheets (ZnO-GO) [95].

Although all the above-mentioned authors also published remarkable studies on hydrothermal synthesis of particles, we cannot avoid mentioning Professor Stanley Whittingham from Binghamton University, who focused his research on hydrothermal synthesis processes for the development of lithium-ion batteries. He actually received the 2019 Chemistry Nobel Prize for his findings. Professor Stanley Whittingham and its collaborators discovered that when lithium ions were held between titanium sulphide plates electricity was generated.

3.2. Types of Particles Generated and Their Applications

Some of the most relevant groups of particles generated by means of hydrothermal synthesis can be seen below [17]:

- Simple oxides such as, for instance, CoO_2, ZnO, CeO_2, TiO_2, ZnO, ZrO_2, CuO, Al_2O_3, In_2O_3, Co_3O_4, etc. Simple oxide particles comprise one of the largest inorganic compound groups.
- Multiple oxide particles (La_2CuO_4, etc.) comprise one of the most important groups with regards to the number of studies and synthesized particles.
- Particles with elements from II to VI: CdS, PbS, ZnS, CuS, NiS_2, Bi_2S_3, CdSe, Bi_2Te_3, $CoSb_3$, PbTe, etc.
- Phosphates, silicates, borates, and carbonate particles ($Zr(PO_4)_3$, $LiFePO_4$, $Li_3Nd_2(BO_3)_3$, Li_2SiO_3, etc.) were and still are of great interest because of their ceramic, optical, piezoelectric, ionic, luminescent, and magnetic properties.

- Fluoride particles with transition metals are particles with great physical, ionic, and magnetic properties ($(TiOF_4)_2$, AlF_3, etc.).
- Fluorine particles, phosphates and fluorine, and carbonates ($M+M(PO_4)F$, $M_3Ln_2(CO_3)_4F$) are often materials with high chemical and thermal stability. They also show great magnetic and electrical properties.
- Tungsten particles either simple or multiple ($M(WO_4)_2$) exhibit great luminescent and electrical properties.
- Molybdenum particles (M_xMoO_4) are closely related to Tungsten and present important optical, magnetic, and electrical properties.
- Metal particles such as Ag or Co.
- Metal oxide particles hybridized with organic compounds. Organic and inorganic hybrid nanoparticles are thought to be the most promising type of materials because exhibit a combination of properties between organic and inorganic polymers (high mechanical resistance, high conductivity, and high electricity resistance) [94]. Figure 8 shows the formation process. At first, and after increasing the temperature from the environmental conditions to the near the critical point, the hydrolysis and dehydration of the metal salt occurs (Mn+), as shown in Equations (1) and (2) of the Section 3. Once the supercritical conditions are reached, organic surface modifiers may form a homogeneous phase with supercritical water. After nucleation has taken place and supercritical conditions have been reached, the dissolved tensioactive compounds are adsorbed into the nucleus (hydrophilic metal oxides). Under these conditions an extremely strong bond is formed on the surface, and the stabilization of the nanoparticles leads to size reduction. At the end of the process, when room temperature is reached again, the organic phase can be easily separated from the water [96].

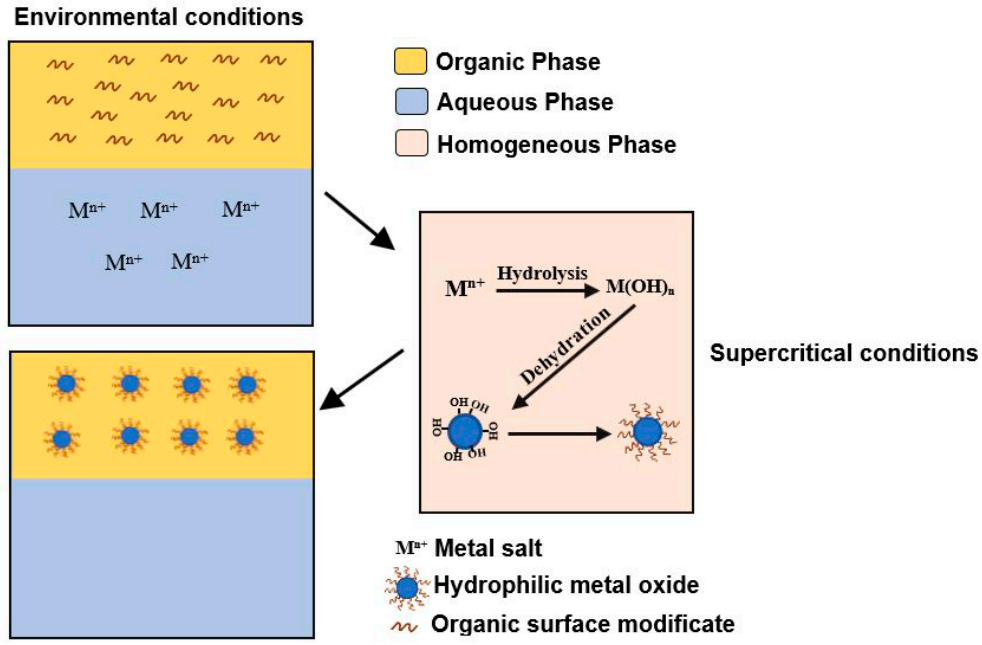

Figure 8. Strategy for the synthesis of metal oxide nanoparticles in a supercritical hydrothermal process assisted by organic ligands.

All the particles described above have or promise to have a great future in many fields of study. The following are particularly prominent:

- Materials: ceramic, for biomedical devices (synthetic bone, joints, or teeth), cutting tools (surgical equipment, etc.), nylon synthesis, etc.

- Electronics: dielectric amplifiers, computer memory components, transformers, electronic ceramic components, capacitors, and other electronic components.
- Medical applications: particularly as cancer treatment drug carriers.
- Catalysis: Fischer–Tropsch reaction, ambience catalysts, etc.
- Power: solar panel screen and cell coating, lithium-ion batteries, etc.

Once the main types of particles that can be generated by hydrothermal procedures are determined, it is important to observe the kind of morphologies that were produced and their evaluation methods.

3.3. Particle Morphology, Types, and Analysis Techniques

The morphology is extremely important with regards to particle functionality. For instance, the different morphologies that were observed in the generation of $LiFePO_4$ particles are enormously interesting for the design of new electric batteries that affect the diffusivity of ion lithium and, therefore, their functionality [97]. It was found that by varying the operating conditions, flat, hexagonal, spherical, porous spheres, prisms, or tetrahedrons can be obtained, as can be seen in Figure 9.

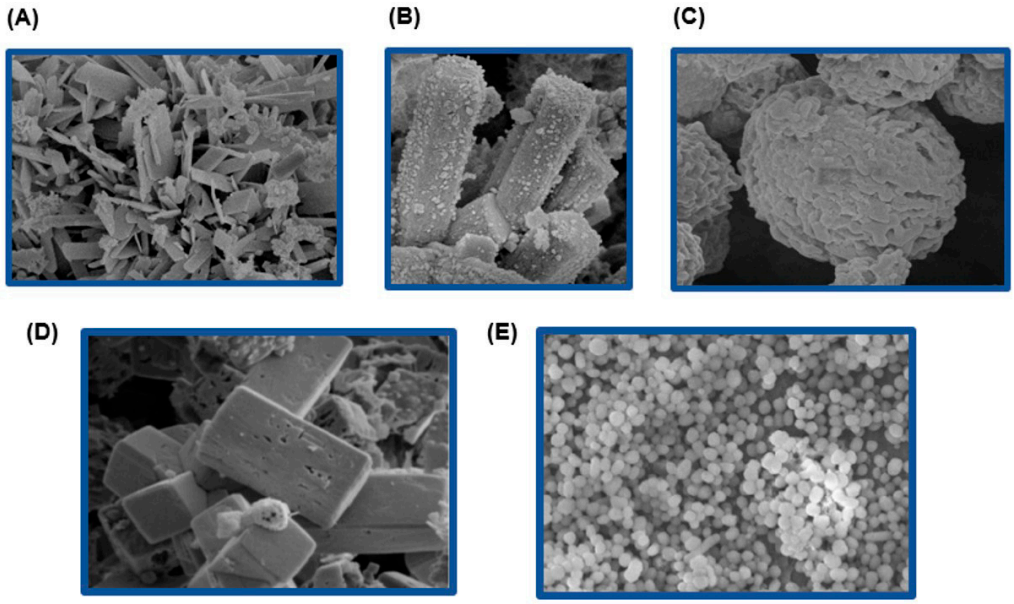

Figure 9. Different crystalline morphologies observed by scanning electron microscopy (SEM) during the hydrothermal synthesis of $LiFePO_4$ particles under different experimental conditions: (**A**) flat plates (**B**) prisms, (**C**) porous spheres, (**D**) tetrahedron, and (**E**) spheres.

Apart from the specific morphologies of $LiFePO_4$ particles, the particles that were generated by hydrothermal synthesis comprise a wide variety of morphologic types, such as tubes, spheres, dots, mushroom shaped, etc. [94].

The products obtained are evaluated through different techniques. From all the techniques, the following stand out for their more generalized use:

- X-ray Diffractometer (XRD) for product characterization. This is a non-destructive technique that allows the analysis of all kinds of samples (fluid, powder, or crystal) and is based on the comparison with known diffraction patterns that are unique to each molecule.
- High Resolution Transmission Electron Microscopy (HRTEM) to analyze the internal structure of the materials at nanometric scale using Fourier transform images.
- Scanning Electron Microscopy (SEM) to analyze particle sizes and morphologies. It is based on the principles of optical microscopy, but the beam of light is replaced by a beam of electrons and, therefore, only the particles surfaces can be analyzed. It is also used to determine composition (Energy Dispersive X-rays Spectroscopy mode).

- Field Emission Scanning Electron Microscopy (FE-SEM) to evaluate particle size and morphology. Like SEM it can only obtain information from the sample surface, although with a higher resolution.
- Fourier-Transform Infrared (FTIR) Spectroscopy to determine the presence of chemical bonds on the nanoparticles' surfaces.

4. Operating Parameters

Particle generation procedures comprise a large number of variables that can be set up to optimize production with regards to their functionality. Such variables have an impact on two essential parameters. On the one hand, crystallization rate and, on the other hand, precursors and generated products solubility. With regards to crystallization rate, Professor Tadafumi Adschiri proved that the rate-determining step in the recrystallization global kinetics is the superficial reaction rate, since diffusivity at conditions near the critical point is very high [16]. With regards to solubility, high values are required for the precursors, while low values are required for the products. Therefore, variations in operating variables should focus on improving the surface reaction rate and the solubility of the reagents and precursors. The variables are as follows:

- Surface modifier: organic molecules such as formic acid, octanoic acid, or hexane, which by forming ligands with metals have an impact on the growth of metal and specifically change the morphology of the particles, generally by reducing their size.
- Operating temperature: Temperature is a variable with an impact on conversion and particle size. Generally, an increment in temperature makes the conversions grow, but also particle size increases since both reaction and crystallization rates are also augmented. There is, therefore, an optimum temperature level that lets us obtain a large number of particles of the desired size.
- Reactor heating rate: In general, a rapid heating rate results in a greater number of crystals cores in a shorter time. This is due to a greater solubility of the precursors in the reaction medium. However, low heating rates, generally result in a gradual generation of crystals cores, which favors a greater distribution of particle sizes. Depending on the kinetics of each specific nanoparticle, a high heating rate may be a limiting factor, i.e., it may control the process when the kinetics are fast, but it would not affect the process when the kinetics are slow. The heating rate is usually reduced by using microreactors or different heating systems. Both aspects will be explained in more detail in Section 5.1.
- pH: pH is an essential factor to consider in hydrothermal synthesis of particles. Acids and basis are normally used to alter pH depending on the solubility of the specific precursors to be used. The pH value can affect the appearance of impurities, as can be observed in the article by Yi-Jie et al. [98], or even be an influent parameter in the modulation of the particles morphology, as can be seen in the article by Xiongjian et al. [99]. That is, depending on the particle to be synthesized, there is a specific optimum pH.
- Residence time: When working under subcritical conditions, reactions are slow. Therefore, the required residence times may be as long as several hours. When working under supercritical conditions the reactions are extremely rapid, and, therefore, residence time is reduced to minutes or even seconds. Exceeding optimum residence time may lead to particle size increments.
- Precursor concentration: Generally, when the concentration of the reagent is low, the sizes of the particles obtained are more regular. However, if the precursor's concentration is really high, a larger number of particles will be produced, although with more irregular sizes since agglutinations may lead to greater size particles.
- Pressure: Pressure, a priori, has no direct effect on particle forming rate. It may, though, affect thermophysical properties, such as solubility, density, etc. It is, therefore, important to work under pressure levels that allow water to remain in its liquid phase or supercritical state at the required operating temperatures.

It is important to specify, therefore, that no optimum value or range of values can be specified for each one of the above explained parameters, since their optimum value will depend on the final particle to be obtained as well as on the precursors used. It must be kept in mind that in some cases, the same particle can be generated while using different reagents.

5. Hydrothermal Reactors

Generation of micro- and nanoparticles by hydrothermal synthesis under such severe conditions requires the use of reactors that can stand high tension and the highly corrosive properties of water under such conditions. For that reason, the materials used to manufacture them are: 300 series stainless steel; superalloys such as Hastelloy, Inconel, and those based mainly on cobalt; and titanium and its alloys [16]. Apart from the construction material, some of these reactors may be fitted with a corrosion protective coating that could be made of gold, silver, platinum, copper, nickel, or quartz among other materials. For the design of the reactors exposed below, there is a very important factor to take into account when working with subcritical water, since the reaction rates are lower than those achieved when operating with supercritical water, because the rate constants decrease drastically in the subcritical zone [100]. Particles can be generated by batch or continuous reactors, each involving different features and advantages depending on the type of study to be carried out (see Table 3).

Table 3. Main differences between batch reactors and continuous flow reactors.

Features	Batch Reactors	Continuous Flow Reactors
Research stage	Initial	Advanced
Operability	Easy handing	Difficult handing
Reaction time	Minutes and even hours	Seconds or a few minutes
Heating time	Long (minutes)	Short to very short (seconds)
Particles size	In the order of a few microns	In the order of nanometers
Process control	Minor operation range	Major operation range

5.1. Batch Reactors

Batch reactors are widely used to produce nanoparticles, mainly because they are often the initial basis of an investigation and are also particularly easy to operate. They normally feature longer reaction times (minutes or even hours) than continuous reactors and have a lower heating rate, since continuous reactors are heated practically instantaneously (the reagents are mixed when the desired temperature is reached).

The most commonly used batch reactors for the hydrothermal processing of advanced nanomaterials are as follows [16]: general purpose autoclaves, Morey type and flat plate seal, stirred reactors, cold-cone seal Tuttlee Roy type, TZM autoclaves, piston cylinder apparatus, belt apparatus, opposed anvil, and opposed diamond anvil. Each one of these reactors has its own characteristics. Batch reactors with a volume between 25 and 1000 mL and the possibility of sample extraction are a frequent and interesting choice, since they allow to obtain multiple data for phase diagrams that cast some insight on the development of the process. Small batch reactors (microreactors) with a volume between 5 and 10 mL are also very interesting and often used, since they prevent any temperature gradients from appearing inside the reactor and allow the implementation of high heating rates to reach the required conditions in just a few seconds. Thus, the data obtained are closer to those obtained with continuous reactors. Professors Arita and Achiri were pioneering supporters of these microreactors and suggested that microreactors with a volume between 5 and 8 mL should be used to avoid slow heating rates and the subsequent temperature gradients [21]. The generation of some of the particles with these reactors, under both subcritical and supercritical conditions, can be seen in Table 4.

Table 4. Particles Generated by Hydrothermal Synthesis in Batch Reactors.

Reactor Volume (mL)	Precursors	T (°C) and P (bar)	Reaction Time	Product	Applications	References
5	$ZrOCl_2$, KOH. Surface modifiers: PHA or PPA	T = 300 and 400; P = 300	10 min	ZrO_2	Highly employed in ceramic materials, biomedical devices and cutting tools, magnetic material products, artificial bone production, artificial joints, artificial teeth, and other pieces of instrument elaboration of watches.	[67]
5	$Zr(OET)_4$ or $Zr(OH)_4$	T= 200–500; P = 380	10 min			[101]
5	$Zr(OH)_4$. Surface modifiers: oleic acids, dodecanoic and 12-aminododecanoic.	T = 400; P =380	10 min			[102]
8.5	Bohemian powder and monocarboxylic acids to favor crystallization and rod formation (hexanoic, octanoic, decanoic, tetradecanoic, and octadecanoic acids).	T = 200–400; P = 300	10 min	ALOOH	Electronics, pharmacy, catalysis, energy storage, and medical applications.	[103]
8.5	Bohemite powder and monocarboxylic acids to favor crystallization and rod formation (hexanoic, octanoic, decanoic, tetradecanoic, and octadecanoic acids).	U.d	U.d			[104]
5	($Al(NO_3)$. Reagents modifiers: hexanal and N-Hexilamina	T = 300; P = 300	10 min			[105]
5	TiO_2 and $Ba(OH)_2$	T = 400; P = 300	10 min	$BaTiO_3$	Non-linear elements, dielectric amplifiers, memory components of electronic computers and groundwater detection devices. In addition, it can also be used to create static electricity in transformers, electronic ceramics, capacitors, and other electronic components.	[106]
5	$Ce(OH)_4$.Surface modifiers: polyvinyl alcohol (PVA) or polyacrylic acid (PAA)	T = 400; P = 300	10 min	CeO_2	Removal of heavy metals from water.	[107]
10	Ce $(OH)_4$ and monocarboxylic acids to improve crystallization (hexanoic, octanoic, decanoic, tetradecanoic, and octadecanoic acids).	T = 400; P = 380	30 min			[108]
5	$Co(CH_3COO)_2{\cdot}4H_2O$ and formic acid as a reducing agent	T = 340, 350, 360, 380, 400 and 420; P = 221	10 min	Co (Metallic)	They are widely used in cement, magnetic fluids, magnetic materials, and batteries, among other uses.	[109]
5	$CoSO_4$ (99%), Al_2SO_4 (55%), and NaOH. Surface modifiers: hexanoic acid and 1-hexylamine	T = 400; P = 380	10 min	$CoAl_2O_4$	They have the potential to be used as pigments in special fields, including UV stabilization of plastics, transparent inks, coating on luminescent materials, etc.	[110]

Table 4. *Cont.*

Reactor Volume (mL)	Precursors	T (°C) and P (bar)	Reaction Time	Product	Applications	References
5	$Co(CH_3COO)_2{\cdot}4H_2O$ Reducing agent: formic acid and methanol	T = 350, 365, 375, 400, 425 and 450; P = 221	U.d	CoO_2	Excellent catalyst for the Fischer-Tropsch reaction. Cobalt nanoparticles have also been used in computer storage devices, due to their high coercivity.	[62]
5	($FeSO_4$); Modifiers: n-decanoic acid ($C_9H_{19}COOH$) or n-decylamine ($C_{10}H_{21}NH_2$).	T = 200; P = 10	10 min	Fe_2O_3 or Fe_3O_4	They are employed in Biology and medicine. Especially in drug carriers to treat cancer.	[111]
5	Metal Salt; Modifiers: oleic acid; Reducing agent: formic acid.	T = 400	10 min	FePt	Information storage: it is the most promising candidate for high density storage.	[112]
5	$GdNO_3$; Modifiers: acid 3,4dihydroxybenzenepropanoic (DHCA) and KOH.	T = 350	10 min	$Gd(OH)_3$	Catalyst: useful in the biomedical field and in neutron capture therapy.	[113]
5	($I(NO_3)_3$ $6H_2O$), (NH_4 VO_3). Modifiers: oleic acid and oleilamina	T = 300, 350 and 400	10 min	$GdVO_4$	They have interesting luminescent and magnetic properties. It can be easily doped with rare earths for different applications such as up-converter or laser.	[114]
5	$Sn(OH)_2$, $In(OH)_3$. Reducing agent: ethanol, formic acid.	T = 410–450; P = 230–400	10–60 min	indium oxide doped whit Tin (ITO)	They are often used as a coating material for display panels, solar cells, and transparent electrodes used in liquid crystal displays (LCD).	[115]
5	$HfCl_4$ and KOH. Modifiers: DHCA.	U.d	10 min	HfO_2	Manufacture of lenses, reflectors, optical waveguides, optical adhesives, and anti-reflective films.	[116]
5	$Al(NO_3)$, $Y(NO_3)$, and KOH. Modifiers: alquilamina (for example, oleilamina, decilamina, dodecilamina, or hexadecilamina).	T = 420;	10 min	YAG	Excellent candidate as host material in solid state lasers	[117]
10	1.2-phenylenediamine and benzoic acid	T = 100–400; P = 1–574	U.d	2-phenylbenzimidazole	They can act as ligands to the transition metals for the modeling of biological systems. Moreover, they can be used to treat parasitic diseases.	[118]

U.d = Unavailable data.

As already mentioned, generally, batch hydrothermal reactions do not quickly reach a supersaturation of the medium due to slow heating rates, which results in the generation of micrometric sized particles [119]. Therefore, heating systems are to be considered as a major factor. The small size of these reactors allows them to be heated by different methods, such as heating blankets [104], microwaves [120], sand baths [121], oil baths [122], etc. Min et al. [123] showed the influence of different heating rates on the particles. Our research group also managed to demonstrate the influence of reactor cooling rates on the crystallinity, morphology, and growth orientation of the microparticles of $LiFePO_4$ obtained by hydrothermal synthesis therefore opening up an interesting field of study in these small reactors [121].

As mentioned above, batch reactors are often used at the initial stages of most research studies, and therefore, most of the authors mentioned in Section 3.1 used them at some point.

5.2. Laboratory Scale Continuous Flow Reactors and Pilot Plants

The studies that were carried out using continuous flow reactors, mainly tubular reactors, are particularly relevant, since they are just one step away from the production of particles at a prospective industrial scale. The main peculiarity of this type of reactors is an improved control on the process, which allows a rapid and continuous synthesis of the particles with relatively minor particle size variations. The main difficulty lies with the mixing of the metal salt and the water, which makes it the main object of current studies. The method used to mix the water with the salt solution is a crucial factor towards the viability of the process, since a rapid generation of homogeneous and functional particles depends largely on this mixing process. Many authors described innovative mixing methods.

In 2006, Professors M. Poliakoff and E. Lester developed a new, optimized reactor mixing system known as the "nozzle reactor", the design of which is based on light absorption imaging (LAI) and computational fluid dynamics (CFD) and the mixing mechanics of which were proven to be excellent [124]. In this case, the two streams do not meet in a mixing point to later on enter the reactor, but, as can be seen in Figure 10, it is inside the reactor where the two streams, the previously heated up to supercritical conditions water stream and the metal salt stream, are mixed by means of a nozzle diffuser. Thus, both streams turn into a very effective mixture with a high Reynolds number because of their different densities.

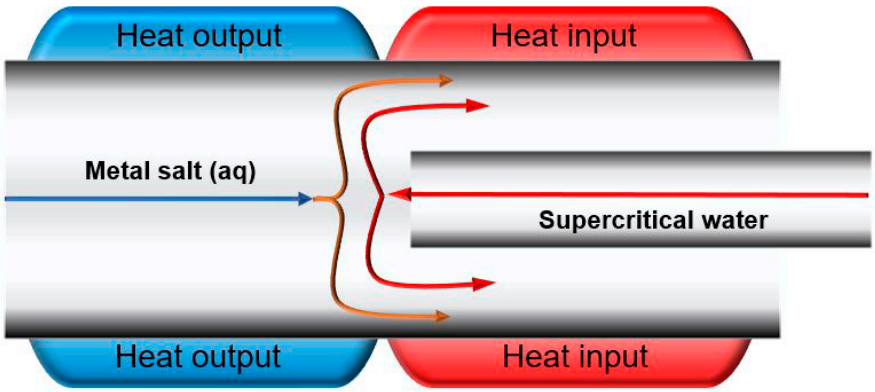

Figure 10. Schematic diagram of the mixture inside the reactor.

Professors Arai and Adschiri were pioneers in producing metal oxides, using a T-shaped mixing system in a continuous reactor, as shown in Figure 11 [125]. The solution of metal salt in supercritical water can be achieved by means of three different settings, just like the Figure shows.

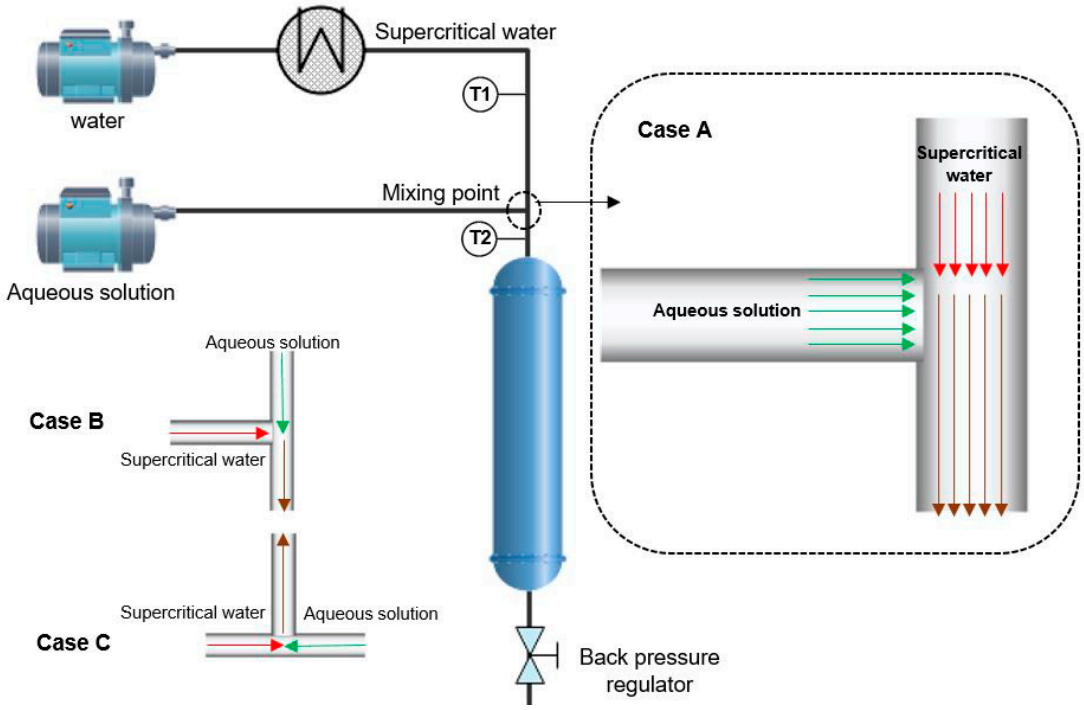

Figure 11. Diagram of a tubular flow reactor used to synthesize nanoparticles.

Other researchers like S. Hong and coworkers (2013) developed reactors where a T-shaped mixing system with different configuration angles was applied. In relation to T-mixers, other researchers reported the use of swirling micromixers (X-shape mixer) with satisfactory results [126].

More recently, a research team from University College London (UCL) developed a highly scalable coaxial or confined jet mixer, which presents several advantages, including that the mixture at ambient temperature being fed with supercritical water takes place almost instantly [127].

As can be seen, mixing hydrodynamics in continuous reactors was the subject of numerous studies, although there is still much ground to be covered, not only in relation to the reactors' hydrodynamics, but also to other aspects that will be further developed in Section 7. It should also be mentioned that, for more information on continuous flow reactors, the especially extensive and rather comprehensive review by Darr et al. [119], entitled "Continuous Hydrothermal Synthesis of Inorganic Nanoparticles: Applications and Future Directions", should be referred to.

5.3. Industrial Scale Reactors

To our knowledge, the number of large-scale industrial plants at a global scale is still rather limited. Because of their peculiarities, two plants stand out among them.

The first one is a plant that was developed by Hanwha Corporation by the end of 2010, in Japan, for the production of $LiFePO_4$. This was the first commercial plant for the continuous supercritical hydrothermal synthesis of $LiFePO_4$. It has a current production capacity of around 1000 tons per year and generates particles of great purity and high functionality [128]. Unfortunately, since Hanwha Corporation is a private enterprise, it is not easy to gain access to any data related to their plant.

The other plant that should be mentioned is the one developed through the SHYMAN project (Sustainable Hydrothermal Manufacturing of Nanomaterials), which is run by Nottingham University with the support received from 17 sponsors across Europe. In 2016, SHYMAN was awarded a European Commission grant worth €10 M, out of which €2 M were intended to build a hydrothermal plant with a production capacity of 100 tons per year. Currently, this plant is located at Promethean Particles company (Nottingham), and it has a production capacity of 1000 tons per year. One of its main

peculiarities is its capacity to produce a wide range of different materials, and for this reason, it is considered the largest multi-material nanoparticle-producing plant worldwide [129].

The plant was developed based on the research work carried out at the University of Nottingham, where the reactor configuration was developed, initially at bench (g/h) and subsequently pilot scale (kg/day), prior to the start of the project. In order to validate the plant and its procedures, a selection of commercial products from different fields were selected as follows: bone materials (such as Hydroxapatite), metal nanoparticles (such as Pt, Ag, Au), medical diagnostics, printed electronics materials (such as ITO), functional lubricants (such as sulphides), ceramic and catalysts nanoadditives for polymers (such as TiO_2 and SiO_2), doped luminescent ceramics (such as YAG:Ce), superhydrophobic materials (such as CeO_2 and SiO_2), and functional polymer additives (e.g., UV-resistant materials like ZnO or flame retardants).

6. Hydrothermal Technology Hybridization

Improving reaction rate and searching for new particles are some of the essential research objectives in this field. They were the ground for numerous studies mainly based on the hybridization of this technology with electrochemistry, mechanochemistry, ultrasounds, and microwaves among others. Below, the most relevant hybrid methods are briefly described.

6.1. Electromechanically Assisted Hydrothermal Synthesis

This technology combines the hydrothermal method with electrochemical treatments and involves the deposit of polycrystalline oxide films on metal electrode substrates [130]. Employing high temperature during hydrothermal processes may deteriorate particles and also demand an extremely high-power consumption. Thus, this method allows to generate thin films under relatively middle temperatures, generally not over 200 °C [65], which allows to cut down on production costs. Figure 12 shows a typical reactor for this method.

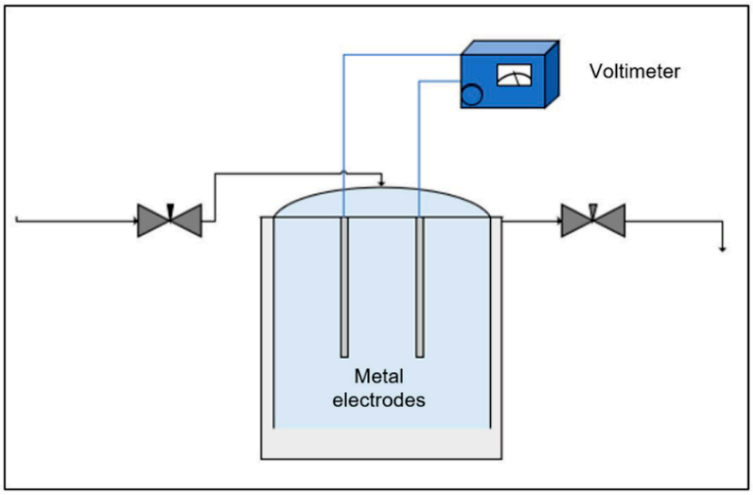

Figure 12. Batch reactor for electrochemically assisted hydrothermal synthesis.

6.2. Mechanochemically Assisted Hydrothermal Synthesis

This method is based on the previous grinding of the precursors followed by a hydrothermal treatment [131,132]. Some of its advantages are its low operating temperatures and a short reaction time when compared to a conventional hydrothermal method. It is intended to produce more regularly shaped and highly crystalline particles than conventional mechanochemical methods.

6.3. Ultrasound-Assisted Hydrothermal Synthesis

This method hybridizes hydrothermal synthesis with ultrasounds to increase reaction kinetics up to two orders or magnitude. Generally, this is achieved by integrating an ultrasound transducer into an autoclave [133], which generates a sonochemical environment that causes chemical changes in the molecules (breaks chemical bonds, causes an excited state, and accelerates electron transfers in chemical reactions), improves crystallization kinetics, and enhances mass transport [130].

6.4. Microwave-Assisted Hydrothermal Synthesis

Microwave-assisted hydrothermal synthesis is a hybrid technology that exhibits unique uniform and rapid heating when compared to conventional hydrothermal methods [120]. The main advantage of this method is its high heating rate that means an increment in crystallization kinetics of 1 or 2 orders of magnitude [130]. According to the literature, this is the most frequently used method at present [134].

7. Landmarks to be Reached

The main difficulties against the consolidation of hydrothermal technology as the method to be used for particle generation were, on the one hand, its high operational costs because of its high temperature requirements and, on the other hand, the need to use equipment that is highly resistant to corrosion, since water under hydrothermal conditions is highly corrosive. Considering that the development of new materials for the construction of more resistant and economic reactors is beyond the scope of this review, we will focus on the need to develop new techniques and methods to cut down on hydrothermal synthesis operational costs:

- Mixing method. In continuous reactors, the method to mix the water with the salt solution is a crucial factor for the viability of the process, as already explained in Section 5.2. This factor determines how rapidly the particles are generated, their homogeneity, and their functionality. It is, therefore, a key factor with regards to process viability and cost effectiveness.
- Hybridization. The hybridization of hydrothermal processes with other industrial processes has been recently explored with the main focus on the reduction of power demand. Professors M. Poliakoff and E. Lester have recently studied the possibility of combining the oxidation processes that take place in supercritical water with hydrothermal synthesis processes, so that the particles can be generated thanks to the large amount of heat that is released from the oxidation reactions under these conditions [135]. This is a very attractive field of study, since many other interesting hybridizations may be conceived.
- Heating and cooling rates. These parameters are scarcely studied, particularly continuous reactors, and their effects on the crystallization and purity of the generated particles confirmed their significance [123]. Since there are closely related to reactor sizing, at least with regards to the heating and cooling stages, they represent a substantial factor in terms of cost efficiency and, subsequently, viability of the process.
- Natural resources. The incorporation of natural resources into the process seems to be gaining a lot of momentum at present. Researchers from Mysore University are currently generating particles using natural plant extracts as surface modifiers and stabilizers. They have coined the term bio-hydrothermal synthesis to describe a new process of this nature [53]. It seems that this research path for synthesizing processes presents a promising future and a large number of articles are expected to focus on it.
- Scaling. Industrial scaling is also a crucial aspect to be studied, particularly since larger productions might enhance cost efficiency. As can be seen throughout this review, this matter is still in its early stages.
- General. If these processes viability is to be improved, in addition to what has already been mentioned, it would also be necessary to develop, on the one hand, new typologies, morphologies,

and particle uses and, on the other hand, to study and develop new reactor typologies with improved hydrodynamics.

- Product purification. Perhaps this is the key point towards the viability of this technology, since the products obtained are in suspension in the water and must be separated from that water. For a future consolidation of this technology, an optimal and economical method to separate the particles from the water is still to be devised.

As can be seen, numerous fields of study have been recently opened and remain so. Such issues are to be fully overcome if this technology is to continue developing, improving, and growing (consolidating).

8. Conclusions

Some industries such as the pharmaceutical, chemical, or material-related industries, among others, need the development of technologies such as the hydrothermal synthesis to obtain a stable production of highly pure crystalline nanoparticles of multiple sizes and shapes.

Hydrothermal synthesis is a definitely thriving, extensive, and heterogeneous field that is constantly evolving and also a promising technology for its high reproducibility and for its capacity to generate pure particles with a narrow variation in size, while highly variable in morphology.

Numerous authors from different parts of the world envisioned a promising future for this technology. They produced extensive studies which mainly focused on the following aspects: reactor development; typologies, morphologies, and usage of particles; particle evaluation methods; operational parameters effect; and hybridization with other technologies, all of which was aimed at either increasing the reaction kinetics or reducing the economic demands of the process. Among all the effects that specific operational parameters have on hydrothermal processes, the authors not only focused on the most common ones, such as pH, pressure, precursor concentration, or temperature, but also other parameters such as reactor heating rates or the addition of many different types of precursors and/or surface modifiers were studied. The main focus was placed on the production of particles that meet morphology, characteristics, and purity requirements.

Regarding the reactors used, most studies were carried out in batch reactors at bench scale, since they are more easily available and/or can be constructed and operated with less trouble. However, several of the studies were carried out in continuous flow at bench and pilot plant scales, and some big projects to scale-up the technology are under progress.

There is still a long road ahead and many landmarks to be reached in the development of this technology. Some of such marks to be mentioned among others are its industrial scaling; a deeper and more thorough study of its reaction kinetics; the development of new and improved flow models to enhance hydrodynamics and to avoid nanoparticle precipitation into the reactors; the design and implementation of an optimized reactor heating method; and, of course, increasing the number and variety of synthesized particles. The studies of the addiction of natural compounds in the process are particularly interesting, as well as the different options to hybridize this technology (electromechanically, mechanochemically, ultrasound or microwave assisted) as the desirable approach to confront and resolve some of the aforementioned challenges.

Author Contributions: Conceptualization, F.R.-J., J.S.-O., J.R.P. and E.J.M.d.l.O.; methodology, F.R.-J., J.S.-O. and J.R.P.; software, F.R.-J.; validation, F.R.-J., J.S.-O., J.R.P. and E.J.M.d.l.O.; formal analysis, F.R.-J., J.S.-O. and J.R.P.; investigation, F.R.-J.; resources, J.S.-O., J.R.P. and E.J.M.d.l.O.; data curation, F.R.-J., J.S.-O. and J.R.P.; writing—original draft preparation, F.R.-J.; writing—review and editing, F.R.-J, J.S.-O., J.R.P. and E.J.M.d.l.O.; visualization, F.R.-J., J.S.-O., J.R.P. and E.J.M.d.l.O.; supervision, J.S.-O., J.R.P. and E.J.M.d.l.O.; project administration, J.S.-O., J.R.P. and E.J.M.d.l.O.; funding acquisition, J.S.-O., J.R.P. and E.J.M.d.l.O. All authors have read and agreed to the published version of the manuscript.

Funding: This research was co-financed by the 2014–2020 ERDF Operational Programme and by the Department of Economy, Knowledge, Business and University of the Regional Government of Andalusia. Project reference: FEDER-UCA18-108297.

Acknowledgments: 2014–2020 ERDF Operational Programme and the Department of Economy, Knowledge, Business and University of the Regional Government of Andalusia. Project reference: FEDER-UCA18-108297.

Conflicts of Interest: The authors declare no conflict of interest. The funders had no role in the design of the study; in the collection, analyses, or interpretation of data; in the writing of the manuscript, or in the decision to publish the results.

References

1. McHugh, M.A.; Krukonis, V.J. *Supercritical Fluid Extraction: Principles and Practice*; Elsevier: Boston, MA, USA, 1986.
2. Cejudo Bastante, C.; Casas Cardoso, L.; Mantell Serrano, C.; Martínez de la Ossa, E.J. Supercritical impregnation of food packaging films to provide antioxidant properties. *J. Supercrit. Fluids* **2017**, *128*, 200–207. [CrossRef]
3. Zizovic, I. Supercritical fluid applications in the design of novel antimicrobial materials. *Molecules* **2020**, *25*, 2491. [CrossRef] [PubMed]
4. Kankala, R.K.; Zhang, Y.S.; Wang, S.B.; Lee, C.H.; Chen, A.Z. Supercritical Fluid Technology: An Emphasis on Drug Delivery and Related Biomedical Applications. *Adv. Healthc. Mater.* **2017**, *6*, 1700433. [CrossRef] [PubMed]
5. Guamán-Balcázar, M.C.; Montes, A.; Fernández-Ponce, M.T.; Casas, L.; Mantell, C.; Pereyra, C.; Martínez de la Ossa, E. Generation of potent antioxidant nanoparticles from mango leaves by supercritical antisolvent extraction. *J. Supercrit. Fluids* **2018**, *138*, 92–101. [CrossRef]
6. Montes, A.; Merino, R.; De Los Santos, D.M.; Pereyra, C.; Martínez De La Ossa, E.J. Micronization of vanillin by rapid expansion of supercritical solutions process. *J. CO_2 Util.* **2017**, *21*, 169–176. [CrossRef]
7. Aymonier, C.; Loppinet-Serani, A.; Reveron, H.; Garrabos, Y.; Cansell, F. Review of supercritical fluids in inorganic materials science. *J. Supercrit. Fluids* **2006**, *38*, 242–251. [CrossRef]
8. Sookwong, P.; Mahatheeranont, S. Supercritical CO_2 extraction of rice bran oil—The technology, manufacture, and applications. *J. Oleo Sci.* **2017**, *66*, 557–564. [CrossRef]
9. Portela Miguelez, J.R.; Nebot Sanz, E.; De La Martinez Ossa, E.; Lopez Bernal, J. Cinetica de oxidacion en agua supercritica. *Ing. Quim.* **1996**, *28*, 147–152.
10. Xie, Y.; Zhou, L.; Cao, H.; Liu, C.; Han, Q.; Hao, W. Reaction condition optimization and degradation pathway in wet oxidation of benzopyrazole revealed by computational and experimental approaches. *J. Hazard. Mater.* **2018**, *351*, 169–176. [CrossRef]
11. Dimitriadis, A.; Bezergianni, S. Hydrothermal liquefaction of various biomass and waste feedstocks for biocrude production: A state of the art review. *Renew. Sustain. Energy Rev.* **2017**, *68*, 113–125. [CrossRef]
12. Perez Bayer, J.F. *Gasificacion de Biomasa: Estudios Teorico Experimentales en Lecho Fijo Equicorriente*; Universidad de Antioquia: Antioquia, Colombia, 2009.
13. Yizhak, M. *Supercritical Water, a Green Solvent: Properties and Uses*, 1st ed.; Wiley: Hoboken, NJ, USA, 2012.
14. Hayashi, H.; Hakuta, Y. Hydrothermal Synthesis of metal oxide nanoparticles in supercritical water. *Materials* **2010**, *3*, 3794–3817. [CrossRef] [PubMed]
15. Byrappa, K.; Ohara, S.; Adschiri, T. Nanoparticles synthesis using supercritical fluid technology—Towards biomedical applications. *Adv. Drug Deliv. Rev.* **2008**, *60*, 299–327. [CrossRef] [PubMed]
16. Byrappa, K.; Adschiri, T. Hydrothermal technology for nanotechnology. *Prog. Cryst. Growth Charact. Mater.* **2007**, *53*, 117–166. [CrossRef]
17. Byrappa, K.; Yoshimura, M. *Handbook of Hridrothermal Technology*, 2nd ed.; Elsevier: Amsterdam, The Netherlands, 2013.
18. Caba, A.; Li, J.; Blood, P.; Chudoba, T.; Lojkowski, W.; Poliakoff, M.; Lester, E. Synthesis of nanoparticulate yttrium aluminum garnet in supercritical water—Ethanol mixtures. *J. Supercrit. Fluids* **2007**, *40*, 284–292.
19. Auxéméry, A.; Frias, B.B.; Smal, E.; Dziadek, K.; Philippot, G.; Legutko, P.; Simonov, M.; Thomas, S.; Adamski, A.; Sadykov, V.; et al. Continuous supercritical solvothermal preparation of nanostructured ceria-zirconia as supports for dry methane reforming catalysts. *J. Supercrit. Fluids* **2020**, *162*, 104855. [CrossRef]
20. Weingärtner, H.; Franck, E.U. Thermodynamics Supercritical Water as a Solvent. *Angew. Chem.* **2005**, *44*, 2672–2692. [CrossRef]

21. Arita, T.; Hitaka, H.; Minami, K.; Naka, T.; Adschiri, T. Synthesis of iron nanoparticle: Challenge to determine the limit of hydrogen reduction in supercritical water. *J. Supercrit. Fluids* **2011**, *57*, 183–189. [CrossRef]
22. Zanella, R. Metodologías para la síntesis de nanopartículas: Controlando forma y tamaño. *Mundo Nano* **2012**, *5*, 69–81. [CrossRef]
23. Nandhini, K.S.S.; Arumanayagam, S.M.T.; Murugakoothan, P.V.P. Synthesis, crystal growth, optical, thermal and mechanical properties of a nonlinear optical single crystal: Ammonium sulfate hydrogen sulphamate (ASHS). *Appl. Phys. A* **2018**, *124*, 1–6.
24. Alivisatos, A.P.; Series, N.; Feb, N. Semiconductor Clusters, Nanocrystals, and Quantum Dots. *Science* **2007**, *271*, 933–937. [CrossRef]
25. Lin, B.; Chen, C.; Kunuku, S.; Chen, T.; Hsiao, T.; Niu, H.; Lee, C. Fe Doped Magnetic Nanodiamonds Made by Ion Implantation as Contrast Agent for MRI. *Sci. Rep.* **2018**, *8*, 1–6. [CrossRef] [PubMed]
26. Okada, S.; Sugime, H.; Hasegawa, K.; Osawa, T.; Kataoka, S. Flame-assisted chemical vapor deposition for continuous gas-phase synthesis of 1-nm-diameter single-wall carbon nanotubes. *Carbon* **2018**, *138*, 1–7. [CrossRef]
27. Kosova, N.; Devyatkina, E. On mechanochemical preparation of materials with enhanced characteristics for lithium batteries. *Solid State Ion.* **2004**, *172*, 181–184. [CrossRef]
28. Fernandez, A.; Caballero, A.; Cedex, E. In Situ EXAFS Study of the Photocatalytic Reduction and Deposition of Gold Titania Colloidal. *J. Phys. Chem.* **1995**, *99*, 3303–3309. [CrossRef]
29. Pal, A.; Shah, S.; Devi, S. Microwave-assisted synthesis of silver nanoparticles using ethanol as a reducing agent Microwave-assisted synthesis of silver nanoparticles using ethanol as a reducing agent. *Mater. Chem. Phys.* **2018**, *114*, 530–532. [CrossRef]
30. Vykoukal, V.; Bursik, J.; Roupcova, P.; Cullen, D.A.; Pinkas, J. Solvothermal hot injection synthesis of core-shell AgNi nanoparticles. *J. Alloys Compd.* **2019**, *770*, 377–385. [CrossRef]
31. Schubert, U.; Hiising, N.; Lorenz, A. Hybrid Inorganic-Organic Materials by Sol-Gel Processing of Organofunctional Metal Alkoxides. *Chem. Mater.* **1995**, *7*, 2010–2027. [CrossRef]
32. He, L.H.; Zhao, Z.W.; Liu, X.H.; Chen, A.L.; Si, X.F. Thermodynamics analysis of $LiFePO_4$ pecipitation from Li-$Fe_{(II)}$-P-H_2O system at 298 K. *Trans. Nonferrous Metals Soc. China* **2012**, *22*, 1766–1770. [CrossRef]
33. Burak, A.Y.; Yildiz, E.; Zubieta, J. pH effect on hydrothermal synthesis of the coordination polymers containing pyrazine-2,3-dicarboxylate: Investigation of thermal stability, luminescence and electrical conductivity properties. *J. Turk. Chem. Soc. Sect. A Chem.* **2020**, *7*, 243–258.
34. Lopez, V.; Minichelli, J.; Case, D.; Karin, R.; Doyle, R.P.; Zubieta, J. Hydrothermal synthesis and structure of a two-dimensional Fe(III)-organodiphosphonate compound, [$Fe(O_3PCH_2C_6H_4CH_2PO_3H)(H_2O)$], and an Expansion of the Harris Notation. *Inorg. Chim. Acta* **2020**, *506*, 119518. [CrossRef]
35. Chung, Y.; Cassidy, E.; Lee, K.; Siu, C.; Huang, Y.; Omenya, F.; Rana, J.; Wiaderek, K.M.; Chernova, N.A.; Chapman, K.W.; et al. Nonstoichiometry and Defects in Hydrothermally Synthesized ϵ-$LiVOPO_4$. *ACS Appl. Energy Mater.* **2019**, *2*, 4792–4800. [CrossRef]
36. Wen, B.; Wang, Q.; Lin, Y.; Chernova, N.A.; Karki, K.; Chung, Y.; Omenya, F.; Sallis, S.; Piper, L.F.J.; Ong, S.P.; et al. Molybdenum Substituted Vanadyl Phosphate ϵ-$VOPO_4$ with Enhanced Two-Electron Transfer Reversibility and Kinetics for Lithium-Ion Batteries. *Chem. Mater.* **2016**, *28*, 3159–3170. [CrossRef]
37. Zhu, B.; Cheng, H.; Ma, J.; Kong, Y.; Komarneni, S. Efficient degradation of rhodamine B by magnetically separable ZnS–$ZnFe_2O_4$ composite with the synergistic effect from persulfate. *Chemosphere* **2019**, *237*, 124547. [CrossRef] [PubMed]
38. Smith Pellizzeri, T.M.; McMillen, C.D.; Kolis, J.W. Alkali Transition-Metal Molybdates: A Stepwise Approach to Geometrically Frustrated Systems. *Eur. J. Inorg. Chem.* **2020**, *26*, 597–600. [CrossRef] [PubMed]
39. Smith Pellizzeri, T.M.; McMillen, C.D.; Wen, Y.; Chumanov, G.; Kolis, J.W. Iron Vanadates Synthesized from Hydrothermal Brines: $Rb_2FeV_6O_{16}$, $Cs_2FeV_6O_{16}$, and $SrFe_3V_{18}O_{38}$. *Eur. J. Inorg. Chem.* **2019**, *42*, 4538–4545. [CrossRef]
40. Liu, Y.; Zhang, Z.; Li, X.Y.; Yang, G.Y. A Ni_{11}-cluster sandwiched phosphotungstate supported by $Ni(H_2O)_5$ group. *Inorg. Chem. Commun.* **2020**, *113*, 107765. [CrossRef]
41. Wang, Y.L.; Yang, G.Y. Two α2-Monozirconium-Substituted Dimeric Silicotungstates: Hydrothermal Synthesis, Structural Characterization and Catalytic Oxidation of Thioethers. *J. Clust. Sci.* **2019**, *30*, 1115–1121. [CrossRef]

42. Liu, B.; Wang, Y.; Shang, S.; Ni, Y.; Zhang, N.; Cao, M.; Hu, C. One-step synthesis of mulberry-shaped TiO_2-Au nanocomposite and its H_2 evolution property under visible light. *Colloids Surf. A Physicochem. Eng. Asp.* **2018**, *553*, 203–209. [CrossRef]
43. Zhang, D.; Qin, J.; Wei, D.; Yang, S.; Wang, S.; Hu, C. Enhancing the CO Preferential Oxidation (CO-PROX) of CuO–CeO_2/Reduced Graphene Oxide (rGO) by Conductive rGO-Wrapping Based on the Interfacial Charge Transfer. *Catal. Lett.* **2018**, *148*, 3454–3466. [CrossRef]
44. Wei, Z.; Zhou, Q.; Wang, J.; Zeng, W. Hydrothermal synthesis of hierarchical WO_3/NiO porous microsphere with enhanced gas sensing performances. *Mater. Lett.* **2020**, *264*, 127383. [CrossRef]
45. Xu, K.; Zhao, W.; Yu, X.; Duan, S.; Zeng, W. Enhanced ethanol sensing performance using Co_3O_4–$ZnSnO_3$ arrays prepared on alumina substrates. *Phys. E Low-Dimens. Syst. Nanostruct.* **2020**, *117*, 113825. [CrossRef]
46. Fu, R.; Wu, X.; Wang, X.; Ma, W.; Yuan, L.; Gao, L.; Huang, K.; Feng, S. Low-temperature hydrothermal fabrication of Fe_3O_4 nanostructured solar selective absorption films. *Appl. Surf. Sci.* **2018**, *458*, 629–637. [CrossRef]
47. Jian, J.; Yuan, L.; Qi, H.; Sun, X.; Zhang, L.; Li, H.; Yuan, H.; Feng, S. Sn-Ni_3S_2 Ultrathin Nanosheets as Efficient Bifunctional Water-Splitting Catalysts with a Large Current Density and Low Overpotential. *ACS Appl. Mater. Interfaces* **2018**, *10*, 40568–40576. [CrossRef] [PubMed]
48. Shi, S.Y.; Chen, L.Y.; Zhao, X.B.; Li, Y.; Zhang, J.; Ren, B.X.; Cui, X.B. pH-Dependent Assembly of Three POM-Based Host–Guest Compounds Constituted by Keggin Polyoxoanions and 4,4′-Bipyridines. *J. Clust. Sci.* **2019**, *30*, 299–310. [CrossRef]
49. Shi, S.Y.; Bai, D.; Chen, L.Y.; Liang, J.Q.; Ma, Y.X.; Jiang, W.; Zhang, J.; Cui, X.B. Synthesis and Characterization of a Novel POM-Based Compound Contained Bi-Capped Bi Keggin Anion and Organic Ligand for Multifunctional Catalytic Property. *J. Clust. Sci.* **2019**, *30*, 661–667. [CrossRef]
50. Meng, L.; Liu, K.; Fu, S.; Wang, L.; Liang, C.; Li, G.; Li, C.; Shi, Z. Microporous Cu metal-organic framework constructed from V-shaped tetracarboxylic ligand for selective separation of C_2H_2/CH_4 and C_2H_2/N_2 at room temperature. *J. Solid State Chem.* **2018**, *265*, 285–290. [CrossRef]
51. Meng, L.; Yang, L.; Chen, C.; Dong, X.; Ren, S.; Li, G.; Li, Y.; Han, Y.; Shi, Z.; Feng, S. Selective Acetylene Adsorption within an Imino-Functionalized Nanocage-Based Metal-Organic Framework. *ACS Appl. Mater. Interfaces* **2020**, *12*, 5999–6006. [CrossRef]
52. Byrappa, S.; Vicas, C.S.; Dhanaraj, N.; Namratha, K.; Keerthana, S.D.; Dey, R.; Byrappa, K. Hydrothermal growth of fine magnetite and ferrite crystals. *J. Cryst. Growth* **2016**, *452*, 111–116. [CrossRef]
53. Zare, M.; Namratha, K.; Thakur, M.S.; Byrappa, K. Biocompatibility Assessment and Photocatalytic Activity of Bio-hydrothermal Synthesis of ZnO Nanoparticles by Thymus vulgaris Leaf Extract. *Mater. Res. Bull.* **2018**, *109*, 49–59. [CrossRef]
54. Ramaswamy, P.; Mandal, S.; Natarajan, S. New open-framework phosphate and phosphite compounds of gallium. *Inorg. Chim. Acta* **2011**, *372*, 136–144. [CrossRef]
55. Sarma, D.; Ramanujachary, K.V.; Stock, N.; Natarajan, S. High-Throughput Study of the Cu(CH3COO)2×H2O−5-Nitroisophthalic Acid−Heterocyclic Ligand System. *Cryst. Growth Des.* **2011**, *11*, 1357–1369. [CrossRef]
56. Nithya, M.; Praveen, K.; Saral sessal, S.; Sathya, U.; Balasubramanian, N.; Pandurangan, A. Green synthesis of α-Fe_2O_3/$BiPO_4$ composite and its biopolymeric beads for enhanced photocatalytic application. *J. Mater. Sci. Mater. Electron.* **2018**, *29*, 14733–14745. [CrossRef]
57. Rajesh, D.; Mahendiran, C.; Suresh, C.; Pandurangan, A.; Maiyalagan, T. Hydrothermal synthesis of three dimensional reduced graphene oxide-multiwalled carbon nanotube hybrids anchored with palladium-cerium oxide nanoparticles for alcohol oxidation reaction. *Int. J. Hydrogen Energy* **2019**, *44*, 4962–4973. [CrossRef]
58. Bhat, T.S.; Kalekar, A.S.; Dalavi, D.S.; Revadekar, C.C.; Khot, A.C.; Dongale, T.D.; Patil, P.S. Hydrothermal synthesis of nanoporous lead selenide thin films: Photoelectrochemical and resistive switching memory applications. *J. Mater. Sci. Mater. Electron.* **2019**, *30*, 17725–17734. [CrossRef]
59. Sankar Ganesh, R.; Patil, V.L.; Durgadevi, E.; Navaneethan, M.; Ponnusamy, S.; Muthamizhchelvan, C.; Kawasaki, S.; Patil, P.S.; Hayakawa, Y. Growth of Fe doped ZnO nanoellipsoids for selective NO2 gas sensing application. *Chem. Phys. Lett.* **2019**, *734*, 136725. [CrossRef]
60. Mazinani, B.; Zalani, N.M.; Sakaki, M.; Yanagisawa, K. Hydrothermal synthesis of mesoporous TiO_2–ZnO nanocomposite for photocatalytic degradation of methylene blue under UV and visible light. *J. Mater. Sci. Mater. Electron.* **2018**, *29*, 11945–11950. [CrossRef]

61. Mejía-Martínez, E.E.; Matamoros-Veloza, Z.; Yanagisawa, K.; Rendón-Ángeles, J.C.; Moreno-Pérez, B. Influence of temperature on hydrothermal hot-pressing of magnesium hydroxyapatite powder. *Bol. Soc. Esp. Ceram. Vidr.* **2018**, *57*, 45–54. [CrossRef]
62. Seong, G.; Adschiri, T. The reductive supercritical hydrothermal process, a novel synthesis method for cobalt nanoparticles: Synthesis and investigation on the reaction mechanism. *Dalt. Trans.* **2014**, *43*, 10778. [CrossRef]
63. Hojo, D.; Ohara, H.; Aida, T.; Seong, G.; Aoki, N.; Takami, S.; Adschiri, T. Supercritical hydrothermal synthesis of highly crystalline lanthanum zirconate nanoparticles. *J. Supercrit. Fluids* **2019**, *143*, 134–138. [CrossRef]
64. Taniguchi, T.; Watanabe, T.; Matsushita, N.; Yoshimura, M. Hydrothermal synthesis of monodisperse $Ce_{0.5}Zr_{0.5}O_2$ metastable solid solution nanocrystals. *Eur. J. Inorg. Chem.* **2009**, *14*, 2054–2057. [CrossRef]
65. Suchanek, W.L.; Yoshimura, M. Preparation of Strontium Titanate Thin Films by the Hydrothermal-Electrochemical Method in a Solution Flow System. *J. Am. Ceram. Soc.* **2005**, *81*, 2864–2868. [CrossRef]
66. Seong, G.; Aida, T.; Nakagawa, Y.; Nanba, T.; Okada, O.; Yoko, A.; Tomai, T.; Takami, S.; Adschiri, T. Fabrication of FeO_x-ZrO_2 nanostructures for automotive three-way catalysts by supercritical hydrothermal synthesis with supercritical CO_2 drying. *J. Supercrit. Fluids* **2019**, *147*, 302–309. [CrossRef]
67. Takigawa, S.; Koshimizu, M.; Noguchi, T.; Aida, T.; Takami, S.; Adschiri, T.; Fujimoto, Y.; Yoko, A.; Seong, G.; Tomai, T.; et al. Synthesis of ZrO_2 nanoparticles for liquid scintillators used in the detection of neutrinoless double beta decay. *J. Radioanal. Nucl. Chem.* **2017**, *314*, 611–615. [CrossRef]
68. Kobayashi, M.; Suzuki, Y.; Goto, T.; Cho, S.H.; Sekino, T.; Asakura, Y.; Yin, S. Low-temperature hydrothermal synthesis and characterization of $SrTiO_3$ photocatalysts for NO_x degradation. *J. Ceram. Soc. Jpn.* **2018**, *126*, 135–138. [CrossRef]
69. Asakura, Y.; Inaguma, Y.; Ueda, K.; Masubuchi, Y.; Yin, S. Synthesis of gallium oxynitride nanoparticles through hydrothermal reaction in the presence of acetylene black and their photocatalytic NO:X decomposition. *Nanoscale* **2018**, *10*, 1837–1844. [CrossRef] [PubMed]
70. Hakuta, Y.; Sue, K.; Takashima, H. Synthesis of praseodymium-ion-doped perovskite nanophosphor in supercritical water. *Mater. Res. Express* **2018**, *5*. [CrossRef]
71. Hakuta, Y.; Takashima, H.; Takesada, M. Hydrothermal synthesis of perovskite metal oxide nanoparticles in supercritical water. *Ferroelectrics* **2019**, *539*, 1–8. [CrossRef]
72. Hirano, M.; Takagi, Y. Phase transition and luminescence properties of $GdTiNbO_6$:Eu^{3+} formed by hydrothermal route. *Mater. Res. Bull.* **2018**, *105*, 13–20. [CrossRef]
73. Hirano, M.; Oda, A.; Takagi, Y. Effect of processing conditions on crystallinity and luminescent characteristics of aeschynite-type complex oxide crystals doped with Dy^{3+} and Eu^{3+}. *J. Ceram. Soc. Jpn.* **2019**, *127*, 570–580. [CrossRef]
74. Orooji, Y.; Ghanbari, M.; Amiri, O.; Salavati-Niasari, M. Facile fabrication of silver iodide/graphitic carbon nitride nanocomposites by notable photo-catalytic performance through sunlight and antimicrobial activity. *J. Hazard. Mater.* **2020**, *389*, 122079. [CrossRef]
75. Aghaei, E.; Haghighi, M. Hydrothermal synthesis of nanostructured Ce-SAPO-34: High-performance and long-lifetime catalyst with various ceria contents for methanol to light olefins conversion. *Microporous Mesoporous Mater.* **2018**, *270*, 227–240. [CrossRef]
76. Bazaga-García, M.; Salcedo, I.R.; Colodrero, R.M.P.; Xanthopoulos, K.; Villemin, D.; Stock, N.; López-González, M.; Del Río, C.; Losilla, E.R.; Cabeza, A.; et al. Layered Lanthanide Sulfophosphonates and Their Proton Conduction Properties in Membrane Electrode Assemblies. *Chem. Mater.* **2019**, *31*, 9625–9634. [CrossRef]
77. Zakharova, G.S.; Schmidt, C.; Ottmann, A.; Mijowska, E.; Klingeler, R. Microwave-assisted hydrothermal synthesis and electrochemical studies of α- and h-MoO_3. *J. Solid State Electrochem.* **2018**, *22*, 3651–3661. [CrossRef]
78. Zakharova, G.S.; Thauer, E.; Wegener, S.A.; Nölke, J.; Zhu, Q.; Klingeler, R. Hydrothermal microwave-assisted synthesis of Li_3VO_4 as an anode for lithium-ion battery. *J. Solid State Electrochem.* **2019**, *23*, 2205–2212. [CrossRef]

79. Bauer, D.; Ashton, T.E.; Groves, A.R.; Dey, A.; Krishnamurthy, S.; Matsumi, N.; Darr, J.A. Continuous Hydrothermal Synthesis of Metal Germanates (M_2GeO_4; M = Co, Mn, Zn) for High-Capacity Negative Electrodes in Li-Ion Batteries. *Energy Technol.* **2020**, *8*, 1–11. [CrossRef]
80. Bauer, D.; Ashton, T.E.; Brett, D.J.L.; Shearing, P.R.; Matsumi, N.; Darr, J.A. Mixed molybdenum and vanadium oxide nanoparticles with excellent high-power performance as Li-ion battery negative electrodes. *Electrochim. Acta* **2019**, *322*, 134695. [CrossRef]
81. Hiley, C.I.; Playford, H.Y.; Fisher, J.M.; Felix, N.C.; Thompsett, D.; Kashtiban, R.J.; Walton, R.I. Pair Distribution Function Analysis of Structural Disorder by Nb^{5+} Inclusion in Ceria: Evidence for Enhanced Oxygen Storage Capacity from Under-Coordinated Oxide. *J. Am. Chem. Soc.* **2018**, *140*, 1588–1591. [CrossRef]
82. Reith, L.; Lienau, K.; Cook, D.S.; Moré, R.; Walton, R.I.; Patzke, G.R. Monitoring the Hydrothermal Growth of Cobalt Spinel Water Oxidation Catalysts: From Preparative History to Catalytic Activity. *Chem. A Eur. J.* **2018**, *24*, 18424–18435. [CrossRef]
83. Clark, I.; Dunne, P.W.; Gomes, R.L.; Lester, E. Continuous hydrothermal synthesis of Ca_2Al-NO_3 layered double hydroxides: The impact of reactor temperature, pressure and NaOH concentration on crystal characteristics. *J. Colloid Interface Sci.* **2017**, *504*, 492–499. [CrossRef]
84. Lester, E.; Aksomaityte, G.; Li, J.; Gomez, S.; Gonzalez-Gonzalez, J.; Poliakoff, M. Controlled continuous hydrothermal synthesis of cobalt oxide (Co_3O_4) nanoparticles. *Prog. Cryst. Growth Charact. Mater.* **2012**, *58*, 3–13. [CrossRef]
85. Skjærvø, S.L.; Wells, K.H.; Sommer, S.; Vu, T.D.; Tolchard, J.R.; Van Beek, W.; Grande, T.; Iversen, B.B.; Einarsrud, M.A. Rationalization of Hydrothermal Synthesis of $NaNbO_3$ by Rapid in Situ Time-Resolved Synchrotron X-ray Diffraction. *Cryst. Growth Des.* **2018**, *18*, 770–774. [CrossRef]
86. Beyer, J.; Mamakhel, A.; Søndergaard-Pedersen, F.; Yu, J.; Iversen, B.B. Continuous flow hydrothermal synthesis of phase pure rutile TiO_2 nanoparticles with a rod-like morphology. *Nanoscale* **2020**, *12*, 2695–2702. [CrossRef] [PubMed]
87. Slostowski, C.; Marre, S.; Bassat, J.M.; Aymonier, C. Synthesis of Cerium oxide-based Nanostructures in Near- and Supercritical Fluids. *J. Supercrit. Fluids* **2013**, *84*, 89–97. [CrossRef]
88. Claverie, M.; Diez-Garcia, M.; Martin, F.; Aymonier, C. Continuous Synthesis of Nanominerals in Supercritical Water. *Chem. A Eur. J.* **2019**, *25*, 5814–5823. [CrossRef]
89. Shekunova, T.O.; Istomin, S.Y.; Mironov, A.V.; Baranchikov, A.E.; Yapryntsev, A.D.; Galstyan, A.A.; Simonenko, N.P.; Gippius, A.A.; Zhurenko, S.V.; Shatalova, T.B.; et al. Crystallization Pathways of Cerium(IV) Phosphates Under Hydrothermal Conditions: A Search for New Phases with a Tunnel Structure. *Eur. J. Inorg. Chem.* **2019**, *2019*, 3242–3248. [CrossRef]
90. Teplonogova, M.A.; Yapryntsev, A.D.; Baranchikov, A.E.; Ivanov, V.K. Selective hydrothermal synthesis of ammonium vanadates(V) and (IV, V). *Transit. Metal Chem.* **2019**, *44*, 25–30. [CrossRef]
91. Yang, C.C.; Jang, J.H.; Jiang, J.R. Comparison electrochemical performances of spherical $LiFePO_4$/C cathode materials at low and high temperatures. *Energy Procedia* **2014**, *61*, 1402–1409. [CrossRef]
92. Keerthi, M.; Manavalan, S.; Chen, S.-M.; Shen, P.-W. A Facile Hydrothermal Synthesis and Electrochemical Properties of Manganese dioxide graphitic Carbon Nitride Nanocomposite toward Highly Sensitive Detection of Nitrite. *J. Electrochem. Soc.* **2019**, *166*, B1245–B1250. [CrossRef]
93. Sakthivel, M.; Sukanya, R.; Chen, S.M. Fabrication of europium doped molybdenum diselenide nanoflower based electrochemical sensor for sensitive detection of diphenylamine in apple juice. *Sens. Actuators B Chem.* **2018**, *273*, 616–626. [CrossRef]
94. Aoki, N.; Hojo, D.; Takami, S.; Adschiri, T. *Environmentally Benign Route for Nanomaterial Synthesis by Using SCW*; Elsevier: Amsterdam, The Netherlands, 2014.
95. Kashinath, L.; Namratha, K.; Byrappa, K. Microwave assisted facile hydrothermal synthesis and characterization of zinc oxide flower grown on graphene oxide sheets for enhanced photodegradation of dyes. *Appl. Surf. Sci.* **2015**, *357*, 1849–1856. [CrossRef]
96. Zhang, B.J.; Ohara, S.; Umetsu, M.; Naka, T.; Hatakeyama, Y. Colloidal Ceria Nanocrystals: A Tailor-Made Crystal Morphology in Supercritical Water. *Adv. Mater.* **2007**, *19*, 203–206. [CrossRef]
97. Yu, F.; Zhang, L.; Li, Y.; An, Y.; Zhu, M.; Dai, B. Mechanism studies of $LiFePO_4$ cathode material: Lithiation/delithiation process, electrochemical modification and synthetic reaction. *RSC Adv.* **2014**, *4*, 54576–54602. [CrossRef]

98. Gu, Y.J.; Li, C.J.; Lv, P.G.; Fu, F.J.; Liu, H.Q.; Ding, J.X.; Wang, Y.M.; Chen, Y.B.; Wang, H.F.; Fan, S.H. Novel synthesis of plate-like $LiFePO_4$ by hydrothermal method. *J. New Mater. Electrochem. Syst.* **2016**, *19*, 33–36. [CrossRef]
99. Li, X.; Xu, L.; Li, X.; Hu, M.; Huang, R.; Huang, C. Oxidant peroxo-synthesized monoclinic $BiVO_4$: Insights into the crystal structure deformation and the thermochromic properties. *J. Alloys Compd.* **2019**, *787*, 666–671. [CrossRef]
100. Adschiri, T.; Hakuta, Y.; Arai, K. Hydrothermal Synthesis of Metal Oxide Fine Particles at Supercritical Conditions. *J. Nanoparticle Res.* **2001**, *3*, 4901–4907. [CrossRef]
101. Taguchi, M.; Takami, S.; Adschiri, T.; Nakane, T.; Sato, K.; Naka, T. Simple and rapid synthesis of ZrO_2 nanoparticles from $Zr(OEt)_4$ and $Zr(OH)_4$ using a hydrothermal method. *CrystEngComm* **2012**, *14*, 2117. [CrossRef]
102. Taguchi, M.; Takami, S.; Adschiri, T.; Nakane, T.; Sato, K.; Naka, T. Synthesis of surface-modified monoclinic ZrO_2 nanoparticles using supercritical water. *CrystEngComm* **2012**, *14*, 2132. [CrossRef]
103. Fujii, T.; Kawasaki, S.; Adschiri, T. Kinetic study of octanoic acid enhanced crystal growth of boehmite under sub- and supercritical hydrothermal conditions. *J. Supercrit. Fluids* **2016**, *118*, 148–152. [CrossRef]
104. Fujii, T.; Kawasaki, S.I.; Suzuki, A.; Adschiri, T. High-Speed Morphology Control of Boehmite Nanoparticles by Supercritical Hydrothermal Treatment with Carboxylic Acids. *Cryst. Growth Des.* **2016**, *16*, 1996–2001. [CrossRef]
105. Mousavand, T.; Ohara, S.; Umetsu, M.; Zhang, J.; Takami, S.; Naka, T.; Adschiri, T. Hydrothermal synthesis and in situ surface modification of boehmite nanoparticles in supercritical water. *J. Supercrit. Fluids* **2007**, *40*, 397–401. [CrossRef]
106. Atashfaraz, M.; Shariaty-Niassar, M.; Ohara, S.; Minami, K.; Umetsu, M.; Naka, T.; Adschiri, T. Effect of titanium dioxide solubility on the formation of $BaTiO_3$ nanoparticles in supercritical water. *Fluid Phase Equilib.* **2007**, *257*, 233–237. [CrossRef]
107. Taguchi, M.; Takami, S.; Adschiri, T.; Nakane, T.; Sato, K.; Naka, T. Supercritical hydrothermal synthesis of hydrophilic polymer-modified water-dispersible CeO_2 nanoparticles. *CrystEngComm* **2011**, *13*, 2841–2848. [CrossRef]
108. Taguchi, M.; Yamamoto, N.; Hojo, D.; Takami, S.; Adschiri, T.; Funazukuri, T.; Naka, T. Synthesis of monocarboxylic acid-modified CeO_2 nanoparticles using supercritical water. *RSC Adv.* **2014**, *4*, 49605–49613. [CrossRef]
109. Seong, G.; Takami, S.; Arita, T.; Minami, K.; Hojo, D.; Yavari, A.R.; Adschiri, T. Supercritical hydrothermal synthesis of metallic cobalt nanoparticles and its thermodynamic analysis. *J. Supercrit. Fluids* **2011**, *60*, 113–120. [CrossRef]
110. Rangappa, D.; Ohara, S.; Naka, T.; Kondo, A.; Ishii, M.; Adschiri, T. Synthesis and organic modification of $CoAl_2O_4$ nanocrystals under supercritical water conditions. *J. Mater. Chem.* **2007**, *17*, 4426. [CrossRef]
111. Takami, S.; Sato, T.; Mousavand, T.; Ohara, S.; Umetsu, M.; Adschiri, T. Hydrothermal synthesis of surface-modified iron oxide nanoparticles. *Mater. Lett.* **2007**, *61*, 4769–4772. [CrossRef]
112. Arita, T.; Hitaka, H.; Minami, K.; Naka, T.; Adschiri, T. Synthesis and Characterization of Surface-modified FePt Nanocrystals by Supercritical Hydrothermal Method. *Chem. Lett.* **2011**, *40*, 588–590. [CrossRef]
113. Singh, V.; Naka, T.; Takami, S.; Sahraneshin, A.; Togashi, T.; Aoki, N.; Hojo, D.; Arita, T.; Adschiri, T. Hydrothermal synthesis of inorganic-organic hybrid gadolinium hydroxide nanoclusters with controlled size and morphology. *Dalt. Trans.* **2013**, *42*, 16176–16184. [CrossRef]
114. Singh, V.; Takami, S.; Aoki, N.; Hojo, D.; Arita, T.; Adschiri, T. Hydrothermal synthesis of luminescent $GdVO_4$:Eu nanoparticles with dispersibility in organic solvents. *J. Nanoparticle Res.* **2014**, *16*, 2378. [CrossRef]
115. Li, H.; Arita, T.; Takami, S.; Adschiri, T. Rapid synthesis of tin-doped indium oxide microcrystals in supercritical water using hydrazine as reducing agent. *Prog. Cryst. Growth Charact. Mater.* **2011**, *57*, 117–126. [CrossRef]
116. Sahraneshin, A.; Asahina, S.; Togashi, T.; Singh, V.; Takami, S.; Hojo, D.; Arita, T.; Minami, K.; Adschiri, T. Surfactant-Assisted Hydrothermal Synthesis of Water-Dispersible Hafnium Oxide Nanoparticles in Highly Alkaline Media. *Cryst. Growth Des.* **2012**, *12*, 5219–5226. [CrossRef]
117. Sahraneshin, A.; Takami, S.; Hojo, D.; Arita, T.; Minami, K.; Adschiri, T. Mechanistic study on the synthesis of one-dimensional yttrium aluminum garnet nanostructures under supercritical hydrothermal conditions in the presence of organic amines. *CrystEngComm* **2012**, *14*, 6085–6092. [CrossRef]

118. Dudd, L.M.; Venardou, E.; Garcia-Verdugo, E.; Licence, P.; Blake, A.J.; Wilson, C.; Poliakoff, M. Synthesis of benzimidazoles in high-temperature water. *Green Chem.* **2003**, *5*, 187–192. [CrossRef]
119. Darr, J.A.; Zhang, J.; Makwana, N.M.; Weng, X. Continuous Hydrothermal Synthesis of Inorganic Nanoparticles: Applications and Future Directions. *Chem. Rev.* **2017**, *117*, 11125–11238. [CrossRef]
120. Mishra, S.; Soren, S.; Debnath, A.K.; Aswal, D.K.; Das, N.; Parhi, P. Rapid microwave—Hydrothermal synthesis of CeO_2 nanoparticles for simultaneous adsorption/photodegradation of organic dyes under visible light. *Optik (Stuttg)* **2018**, *169*, 125–136. [CrossRef]
121. Ruiz-Jorge, F.; Benítez, A.; Fernández-García, S.; Sánchez-Oneto, J.; Portela, J.R. Effect of Fast Heating and Cooling in the Hydrothermal Synthesis on $LiFePO_4$ Microparticles. *Ind. Eng. Chem. Res.* **2020**, *59*, 9318–9327. [CrossRef]
122. Qin, X.; Wang, X.; Xiang, H.; Xie, J.; Li, J.; Zhou, Y. Mechanism for hydrothermal synthesis of $LiFePO_4$ platelets as cathode material for lithium-ion batteries. *J. Phys. Chem. C* **2010**, *114*, 16806–16812. [CrossRef]
123. Min, C.; Ou, X.; Shi, Z.; Liang, G.; Wang, L. Effects of heating rate on morphology and performance of lithium iron phosphate synthesized by hydrothermal route in organic-free solution. *Ionics* **2011**, *24*, 1285–1292. [CrossRef]
124. Lester, E.; Blood, P.; Denyer, J.; Giddings, D.; Azzopardi, B.; Poliakoff, M. Reaction engineering: The supercritical water hydrothermal synthesis of nano-particles. *J. Supercrit. Fluids* **2006**, *37*, 209–214. [CrossRef]
125. Sugioka, K.I.; Ozawa, K.; Kubo, M.; Tsukada, T.; Takami, S.; Adschiri, T.; Sugimoto, K.; Takenaka, N.; Saito, Y. Relationship between size distribution of synthesized nanoparticles and flow and thermal fields in a flow-type reactor for supercritical hydrothermal synthesis. *J. Supercrit. Fluids* **2016**, *109*, 43–50. [CrossRef]
126. Zielke, P.; Xu, Y.; Simonsen, S.B.; Norby, P.; Kiebach, R. Simulation, design and proof-of-concept of a two-stage continuous hydrothermal flow synthesis reactor for synthesis of functionalized nano-sized inorganic composite materials. *J. Supercrit. Fluids* **2016**, *117*, 1–12. [CrossRef]
127. Gruar, R.I.; Tighe, C.J.; Darr, J.A. Scaling-up a confined jet reactor for the continuous hydrothermal manufacture of nanomaterials. *Ind. Eng. Chem. Res.* **2013**, *52*, 5270–5281. [CrossRef]
128. Adschiri, T.; Lee, Y.W.; Goto, M.; Takami, S. Green materials synthesis with supercritical water. *Green Chem.* **2011**, *13*, 1380–1390. [CrossRef]
129. Caramazana, P.; Dunne, P.; Gimeno-Fabra, M.; McKechnie, J.; Lester, E. A review of the environmental impact of nanomaterial synthesis using continuous flow hydrothermal synthesis. *Curr. Opin. Green Sustain. Chem.* **2018**, *12*, 57–62. [CrossRef]
130. Shandilya, M.; Rai, R.; Singh, J. Review: Hydrothermal technology for smart materials. *Adv. Appl. Ceram.* **2016**, *115*, 354–376. [CrossRef]
131. Suchanek, W.L.; Shuk, P.; Byrappa, K.; Riman, R.E.; TenHuisen, K.S.; Janas, V.F. Mechanochemical-hydrothermal synthesis of carbonated apatite powders at room temperature. *Biomaterials* **2002**, *23*, 699–710. [CrossRef]
132. Zhang, F.; Hou, W. Mechano-hydrothermal preparation of Li-Al-OH layered double hydroxides. *Solid State Sci.* **2018**, *79*, 93–98. [CrossRef]
133. Schiedeck, F.; Morita, T. Ultrasonic-assisted hydrothermal deposition of ferroelectric $PbZrO_3$ thin film on NiTi-based superelastic shape memory alloys. *J. Electroceram.* **2012**, *28*, 45–52. [CrossRef]
134. Mohammadi, E.; Aliofkhazraei, M.; Hasanpoor, M.; Chipara, M. Hierarchical and Complex ZnO Nanostructures by Microwave-Assisted Synthesis: Morphologies, Growth Mechanism and Classification. *Crit. Rev. Solid State Mater. Sci.* **2018**, *43*, 475–541. [CrossRef]
135. Al-atta, A.; Huddle, T.; García, Y.; Mato, F.; García-serna, J.; Cocero, M.J.; Gomes, R.; Lester, E. A techno-economic assessment of the potential for combining supercritical water oxidation with 'in-situ' hydrothermal synthesis of nanocatalysts using a counter current mixing reactor. *Chem. Eng. J.* **2018**, *344*, 431–440. [CrossRef]